

# DETERMINATION OF THE SODIUM TEMPERATURE COEFFICIENT OF REACTIVITY

by

Quinton Scott Beaulieu

A thesis

submitted in partial fulfillment

of the requirements for the degree of

Master of Science in Nuclear Science and Engineering

Idaho State University

December 2016

To the Graduate Faculty:

The members of the committee appointed to examine the thesis of Quinton Beaulieu find it satisfactory and recommend that it be accepted.

---

Dr. Chad Pope,  
Major Advisor

---

Dr. George Imel,  
Committee Member

---

Dr. Seyed Mousavinezhad,  
Graduate Faculty Representative

### **Acknowledgements**

I would like to thank all of the nuclear engineering professors at Idaho State University for their continued support and tutelage. I would especially like to thank Dr. Chad Pope for his support and encouragement throughout my career.

Lastly, but certainly not least, I would like to thank my wife Jourdin for her unyielding support in all of my ventures.

## **Vitae**

Quinton Beaulieu was born in Henderson, Nevada in July of 1993. He completed his Bachelors of Science at Idaho State University in 2015, and began working towards a Master's of Science at the same institution. During his Bachelors studies, he had the privilege to intern at Idaho National Laboratory for Battelle Energy Alliance.

## Table of Contents

List of Figures .....	v
List of Tables .....	vi
Abstract .....	vii
Literature Review.....	1
Introduction.....	3
Sodium Issue in Current Model .....	10
Theory .....	13
Modeling.....	21
Dimensions .....	23
Materials .....	24
Gradient.....	32
Results.....	36
Conclusion .....	39
References.....	40
Appendix.....	41
A. Additional Material Data for Inner Core .....	41
B. Results of Density and Cross-Sectional Adjustment .....	44
C. MCNP Input File – Gradient at 420°C .....	44

## List of Figures

Figure 1. EBR-II cutaway view. ....	6
Figure 2. EBR-II Element Bundle with Wire Wraps <sup>(9)</sup> .....	7
Figure 3. EBR-II Sub-assembly Geometry (Bottom-to-Top) <sup>(9)</sup> .....	9
Figure 4. Core Loading for EBR-II with Sub-Assembly Key .....	9
Figure 5. Simplified Model.....	13
Figure 6. EBR-II Core Loading During Run138B <sup>(6)</sup> .....	14
Figure 7. Example of Doppler Broadening.....	16
Figure 8. Energy Flux Spectrum of EBR-II.....	17
Figure 9. Flux Map of EBR-II <sup>(0)</sup> .....	21
Figure 10. Plan View of Simplified Model.....	22
Figure 11. Elevation View of Simplified Model. ....	23
Figure 12. Side View of Simplified Model with Gradient.....	32
Figure 13. Axial Temperature Gradient 358°C to 420°C. ....	33
Figure 14. Radial Temperature Gradient 358°C to 420°C.....	34

Figure 15. Axial Temperature Gradient 358°C to 368°C.....	34
Figure 16. Radial Temperature Gradient 358°C to 368°C.....	35
Figure 17. Gradient Temperatures from 358°C to 420°C.....	35
Figure 18. Gradient Temperatures from 358°C to 368°C.....	35
Figure 19. <sup>238</sup> U Cross-Section at 23°C vs. <sup>238</sup> U Cross-Section at 2,226°C near 10eV .....	36

## List of Tables

Table 1. U-5Fs Composition and Weight Percent. ....	5
Table 2. Dimensions of Simplified Model.....	24
Table 3. Volume Fractions for Materials.....	25
Table 4. Sodium Density at Different Temperatures. ....	25
Table 5. Material Data for Inner Core. ....	26
Table 6. Material Data for Blanket Region.....	27
Table 7. Material Data for Stainless Steel Reflector.....	28
Table 8. Material Data for Upper and Lower Extensions.....	29
Table 9. Material Data for Upper Extension Inner Core. ....	30
Table 10. Atom Densities of Sodium and <sup>235</sup> U.....	31
Table 11. Calculated Model Results. ....	37
Table 12. Calculated Results.....	38

## Abstract

This project determined the sodium temperature coefficient of reactivity for EBR-II using the core configuration from a specific experiment. This involved taking a detailed MCNP model that was prepared for a reactor physics benchmark handbook and converting it into a simplified model. Once the simplified model was constructed, a sodium temperature gradient was applied across the model. The gradient was determined by the flux profile in the reactor, which is assumed to be similar to a cylindrical reactor. This gradient is represented by the sodium density in the core. The sodium temperature gradient has adjusted densities and cross-sections modified by NJOY to calculate the reactivity of the temperature change ( $\Delta k$ ).

The reactivity change of the core was calculated for two configurations: one was a bulk-to-bulk model, where the sodium temperature remains constant throughout the core, but increases from model to model. The other was a gradient-to-gradient model, where a temperature gradient is applied to the model, and the temperatures of each gradient increase model to model. The bulk-to-bulk model calculation was very uncertain, with a 42% difference from published literature, whereas the gradient-to-gradient model gave a value of  $-4.00\text{E-}04 \Delta k$  compared to the published value of  $-4.15\text{E-}04 \Delta k$  using a temperature difference of  $52^\circ\text{C}$ . The sodium temperature coefficient of reactivity was calculated to be  $-7.69\text{E-}06 \Delta k/^\circ\text{C}$ .

## Literature Review

For this project, a solid technical basis was needed for all steps, from the type of code used to the calculations for the sodium density and gradient. Additional useful information was the specifics of how the EBR-II core was constructed, as well as flux and power information. In addition, information on Doppler broadening as well as verification that the isotopes used in this project are valid were needed. Finally, a temperature coefficient for sodium was useful in determining if the calculated result from this project is valid.

Reference 1 showed that MCNP was applicable for this project, since it covers the ranges of energies used, as well as it can be used to calculate  $k_{\text{eff}}$  eigenvalues. MCNP stands for Monte Carlo N-Particle, and was developed by Los Alamos National Laboratory. It allows neutron energies from  $10^{-11}$  MeV to 20MeV for all isotopes, and is continuous energy. Information on the ENDF library was useful because many of the cross-sections of isotopes in this project will have to be manipulated for different temperatures, and continuous-energy allows for that.

Reference 2 gave information on a program called NJOY. NJOY is used to produce multi-group cross-sections at different temperatures to be used in the model. Doppler broadening was used extensively to adjust many cross-sections to the temperature in the core.

Reference 3 gave assurance that the ENDF library is up-to-date for the main isotope of this project. It describes how there were differences in the JENDL-3.2 and ENDF/B-VI libraries on how elastic scattering was calculated, and whether or not either method was

correct. The cross sections were recalculated, and the new results included in the latest JENDL-3.3 library.

The equation used for the calculation of the sodium density is taken from Reference 4. In addition, verification is shown that will reduce the likelihood of computational error within the model.

Reference 5 is the only published literature that gives values for the coefficients of reactivity that are distinct from one another, and includes the methodology behind how the calculations of those coefficients were performed. This means that sodium can be singled out and determined, as well as other parameters of interest, such as Doppler broadening. This was useful because this project determined a unique sodium density coefficient of reactivity that was compared to the existing value.

The material data, as well as geometric dimensions, were taken from the Reference 6. This document gives homogenized material data, as well as the volume and dimensions over which that material was homogenized, which was useful in constructing a simplified model. While there are discrepancies between this documents' dimensions and the dimensions found in the engineering drawings, changes and simplifications made in the model from this document were

Information on flux profiles, as well as another value for the mass of uranium-235 in the core were taken from Reference 7. Both of these data are used to verify that the core, while simplified, is a faithful recreation of EBR-II.

## Introduction

A simple model of EBR-II was constructed, with a temperature gradient to simulate the heat flow from the center of the core. MCNP was used to calculate the criticality eigenvalue  $k$ , which was compared to the criticality eigenvalue of the same model with the sodium temperature for all regions at the bulk sodium temperature. This  $\Delta k$  value showed the reactivity from the sodium as temperature increases within the core.

Once the  $\Delta k$  value was calculated, it was compared to the sodium temperature coefficient of reactivity, given by A Study of the Temperature Coefficients of Reactivity for EBR-II Run 93<sup>(5)</sup>. As defined in Section V, “The reactivity changes resulting from the immediate effects of energy production are called prompt reactivity feedback<sup>(5)</sup>.” Lamarsh<sup>(8)</sup> gives a definition of a temperature coefficient of reactivity as “...the extent to which the reactivity is affected by changes in temperature...” Equation 1 shows the relation for a temperature reactivity coefficient.

$$\alpha_T = \frac{d\rho}{dT} \quad \text{Equation 1}$$

Where  $\rho$  is the reactivity of the system, and  $T$  is the temperature. The definition of reactivity in terms of  $k$  is given in Equation 2.

$$\rho = \frac{k-1}{k} = 1 - \frac{1}{k} \quad \text{Equation 2}$$

Equation 2 can be substituted into Equation 1 to produce Equation 3, shown below.

$$\alpha_T = \frac{d\left(1 - \frac{1}{k}\right)}{dT} \quad \text{Equation 3}$$

If Equation 3 is differentiated, it gives Equation 4 below.

$$\alpha_T = \frac{1}{k^2} \frac{dk}{dT} \quad \text{Equation 4}$$

However, if the assumption is made that most reactivity changes are going to happen when  $k$  is close to unity ( $k=1$ ), then Equation 4 can be simplified to Equation 5.

$$\alpha_T = \frac{1}{k} \frac{dk}{dT} \quad \text{Equation 5}$$

Equation 5 is the definition most often used when discussing temperature coefficients<sup>(8)</sup>. It is important to note that for a single reactor, there could be hundreds of different individual temperature coefficients, and that these combine to form the total temperature coefficient of the reactor. Even then, many regions within the reactor could have vastly different reactivity coefficients depending on materials and temperature changes in those regions.

For reactivity coefficients, the sign of  $\alpha$  is important, because it determines whether or not the reactor will increase or decrease in power when the temperature is increased. If  $\alpha_T$  is negative, then the increasing temperature of the reactor leads to a decrease in reactivity, which means that the reactor power will decrease, if one assumes the change is happening from unity. However, if the temperature of the reactor decreases, this will lead to an increase in reactivity of the reactor, which would lead to an increase in power, given a critical reactor.

For EBR-II, the sodium temperature coefficient of reactivity was negative and given in quantities with units of  $\Delta k/^\circ\text{C}$ . This was used to calculate the change in reactivity of the core, based solely on increasing temperature. For instance, if the temperature in the centerline assembly increased by  $30^\circ\text{C}$ , and the total reactivity coefficient for that assembly was  $-0.001 \Delta k/^\circ\text{C}$ , the overall expected change in reactivity would be  $-0.03 \Delta k$ . While

there are several reactivity feedback mechanisms in EBR-II, only two were of interest for this project: the thermal expansion of the sodium, and the Doppler effect. These two values were used to determine the accuracy of the  $\Delta k$  value calculated from the models.

Experimental Breeder Reactor II (EBR-II) was a sodium-cooled, pool-type fast reactor with metallic fuel (Figure 1). EBR-II had an operating power of 62.5 MW. It operated from 1964 through 1994, and was part of the Integral Fast Reactor program in the 1980's and 1990's. This program sought to demonstrate a closed fuel cycle with a fast reactor using and reusing the processed fuel. The reactor itself sat inside a large pool of liquid sodium which was used as the coolant for the reactor as well. The metallic fuel was called U-5 fission because it was composed of uranium, with 5% content being made up of fission<sup>A</sup>. The composition of the uranium and fission are given in Table 1.

Table 1. U-5Fs Composition and Weight Percent.

Material	Weight %
Uranium	95.0
Zirconium	0.01
Molybdenum	2.46
Ruthenium	1.96
Rhodium	0.28
Palladium	0.19
Niobium	0.01

---

<sup>A</sup> Fission was developed to imitate the behavior of fission products.

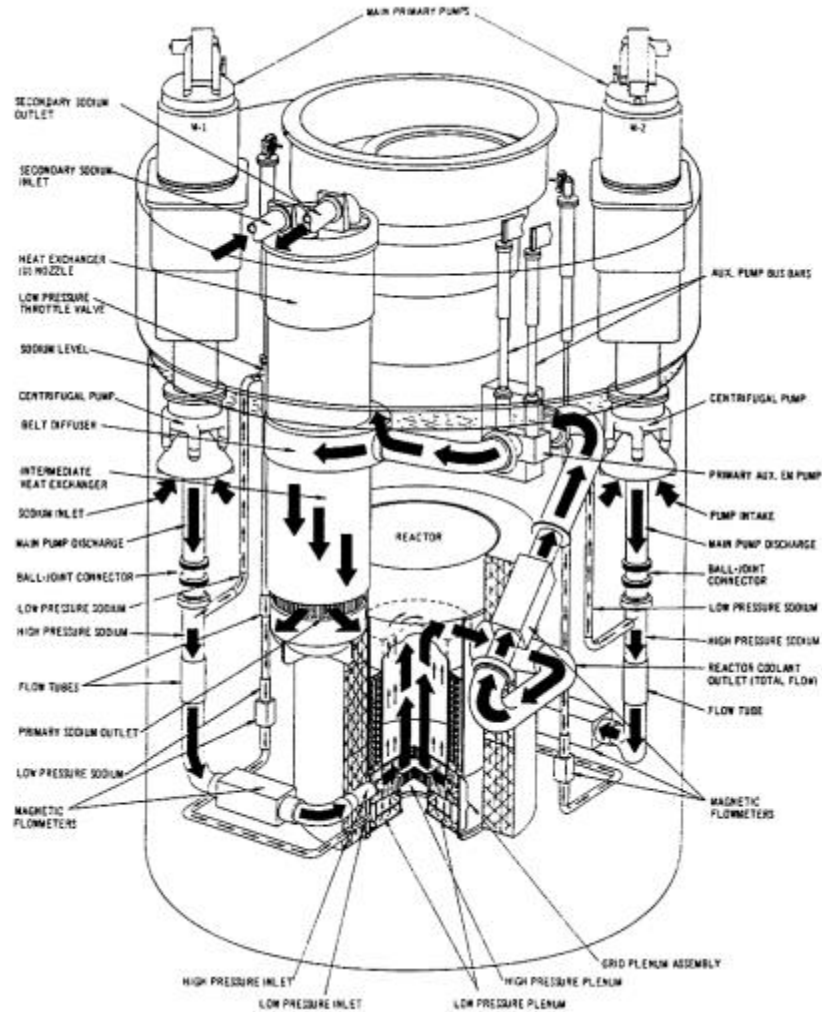


Figure 1. EBR-II cutaway view.

EBR-II consisted of 637 hexagonal sub-assemblies with several different types of sub-assemblies. The outer hexagonal duct housed the entire sub-assembly that was divided into three parts: the upper extension, core region, and lower extension. Both extensions were made of stainless steel flow channels that allowed molten sodium to flow through them. Though there are quite a few different types of sub-assembly, the most important for this project were drivers, high worth controls, stainless steel reflectors, and blankets. Drivers were the fueled rods, with 13.5 inch fuel slugs of 64 a/o  $^{235}\text{U}$  with an argon-helium mix plenum gas area above, encased in 91 elements, as shown in Figure 2.



Figure 2. EBR-II Element Bundle with Wire Wraps<sup>(9)</sup>.

The high worth control rods were similar to a driver, but they only had 61 elements in the core region, and they also had six boron carbide slugs in the upper extension that were used as neutron poison. The stainless steel reflectors were essentially sodium flow channel throughout the entire sub-assembly length, including the core region which had no fuel elements. The blankets had 19 elements that ran the much longer than the driver fuel elements (60 inches), and were filled with depleted uranium. This increased the mass of these sub-assemblies substantially. The general geometry of each sub-assembly is shown in Figure 3.



Figure 3. EBR-II Sub-assembly Geometry (Bottom-to-Top)<sup>(9)</sup>.

These sub-assemblies were divided into three radial sections: the inner core, the reflector, and the outer blanket core. Figure 4 shows the core loading for EBR-II.

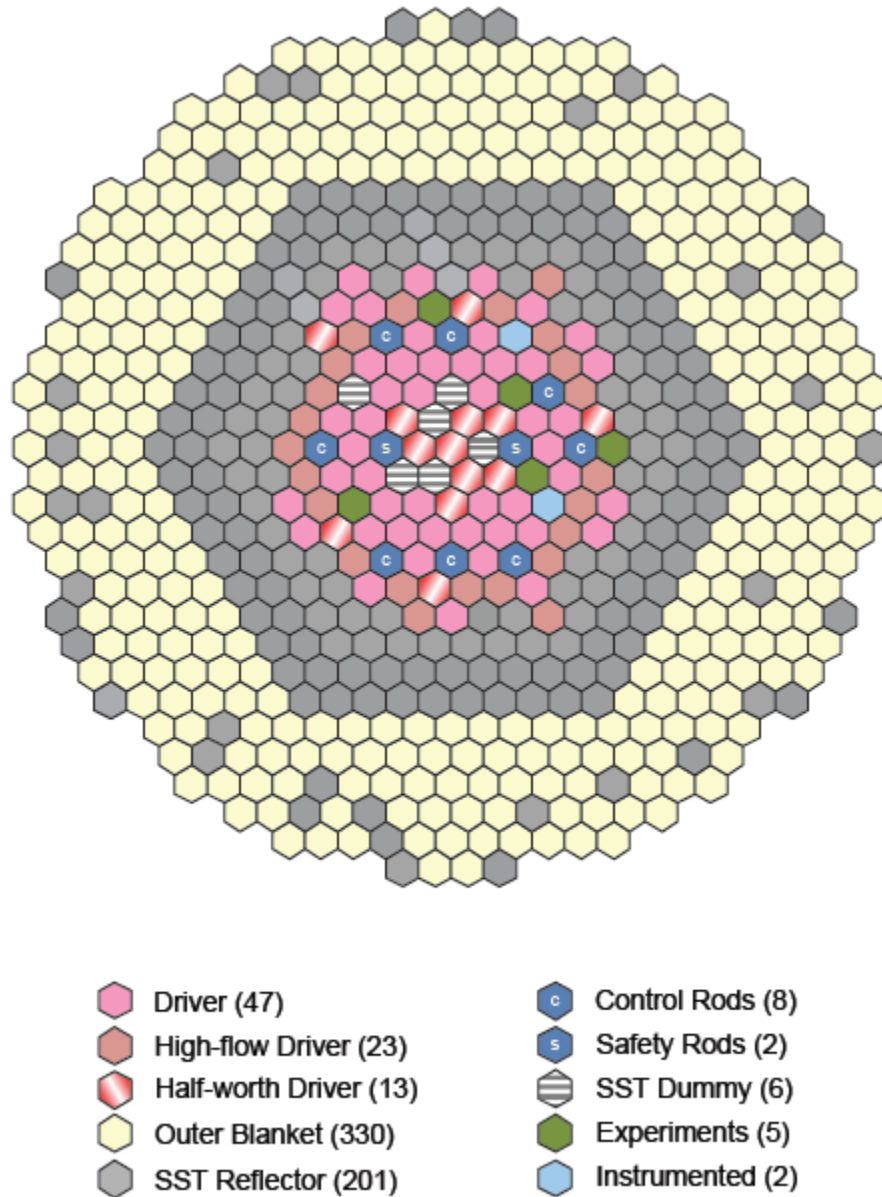


Figure 4. Core Loading for EBR-II with Sub-Assembly Key

The inner core had mostly driver fuel sub-assemblies, but also included high worth control rods and safeties which could be used to control reactivity. The safeties (which

had a fuel loading similar to high worth controls but no boron carbide added) had a binary system, where, if they were inserted, the reactor could achieve criticality. But, without insertion, the reactor did not have enough excess reactivity to achieve criticality. The high worth control rods were used to adjust reactivity while at critical. One high worth control rod would be used as a tuning rod and small adjustments could be made for small changes of reactivity. When the worth of that rod was used up during a run, the rest of the high worth control rods would be banked, meaning they would all be inserted or removed a small amount, and the single tuning rod would be readjusted.

## Sodium Issue in Current Model

The bulk sodium temperature of EBR-II was measured during normal operations, and was kept constant by heaters in the sodium pool. The heaters only kept the sodium at bulk temperature so that the sodium would not return to a solid, and were not used during operation. However, as sodium moved through fueled assemblies, the heat produced conducted into the sodium coolant and out of the core where it was used to produce electric power. The sodium coolant that flowed through these assemblies was a higher temperature due to the heat produced from the fuel. This both decreased sodium density and changed the cross-sections of sodium through Doppler broadening.

The reactor system design description <sup>(7)</sup> for EBR-II has qualitative data on whether or not the sodium density and cross-sections changes would produce a positive or negative reactivity feedback.

“[The second most important reactivity feedback mechanism is]...*The temperature of the sodium in the core increases with increase in reactor power, which decreases the density*

*of the sodium. This reduces the neutron moderating effects of the sodium and contributes to the negative reactivity in the reactor.*

*“[The seventh most important reactivity feedback mechanism is]...The Doppler Effect produces a small increase in positive reactivity with increase in the EBR-II reactor temperature. However, this small reactivity increase is more than compensated for by the negative reactivity effects of decreased fuel and fuel axial expansion.”*

A model for the reactor core was created using a matrix laboratory (MATLAB) code called MICKA, created by Edward Lum<sup>(B)</sup>. This code imports all of the needed dimensional, material, and positional information for the core and creates an MCNP input file with the correct formatting. Because of its versatility, the code includes all of the individual fuel pins within each sub-assembly, as well as the exact location of each pin and sub-assembly within the core. MICKA also calculates the material densities of each isotope within the model based on the burn-up data from a document from Argonne National Laboratory<sup>(6)</sup>. The detailed model includes 91 sub-assemblies in the inner core, which include drivers, control rods, dummies, reflectors, and experiments. Each of these sub-assemblies are hexagonal in shape, and made up of fueled rods, poison rods, and stainless steel and sodium flow channel areas in the upper and lower portions, all with individual impurities and uncertainties.

The MICKA model uses a bulk sodium temperature for all sodium in the core. This project created a simplified model of the EBR-II core specific to the Run 138B

---

<sup>B</sup> MICKA stands for MCNP Input Card and K-CODE Architect, and is a program developed by Edward Lum to assist with the Reactor Physics Benchmark for EBR-II.

configuration, and then divided it into distinct sections where the temperature of the sodium in the core was increased to better reflect the fact that it heated up due to the fuel. This temperature gradient shows the effect of increasing sodium temperature within the core.

For the simplified model, only nominal measurements and isotopes that are most important to  $k$  were included. The simplified model was a large hexagonal prism that is divided into radial regions. The three regions represent the outer core made up of mostly blanket sub-assemblies, a reflector region made up of mostly stainless steel dummy sub-assemblies, and the inner core that included mostly fueled sub-assemblies of various types. The inner core is the only region in the reactor that produced significant power and was the only region that will have a sodium temperature gradient applied. The top-most and bottom-most prisms of each region are made up of a stainless steel and sodium smear which represented the upper and lower extensions within each sub-assembly. The middle and bottom sections of the blanket region are made up of depleted uranium, stainless steel, and sodium. The middle section of the reflector region will be made up of stainless steel. An example of the simplified core is shown in Figure 5.

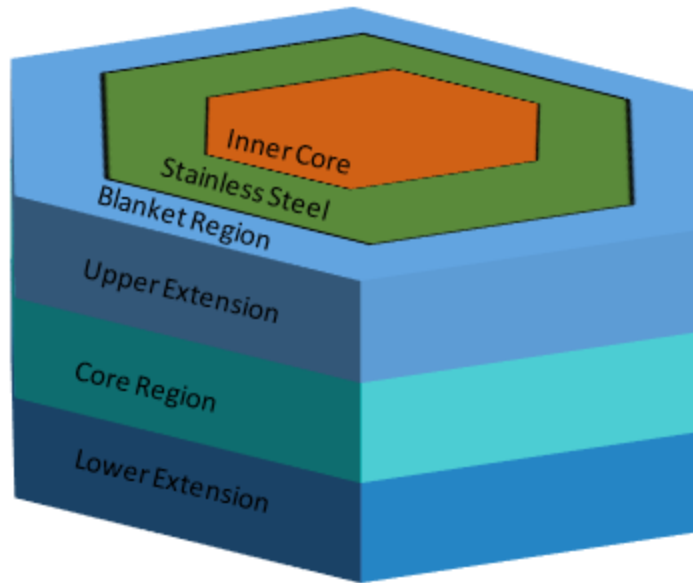


Figure 5. Simplified Model.

## Theory

The simplified EBR-II model used fuel which were nearly beginning of life (BoL). In the EBR-II model used to simulate Run 138B, each sub-assembly had its own burn-up, and therefore its own fissile content. The Neutronics Benchmark Specifications for EBR-II Shutdown Heat Removal Test SHRT-45R – Revision 1<sup>(6)</sup> gives the compositional breakdown for each fueled sub-assembly in the core. Sub-assemblies were chosen from this document to represent each fueled region of the simplified model. The sub-assembly with ID C2893E was chosen to represent BoL driver fuel in the inner core as it was the lowest burned sub-assembly in the core at that time. Its burn-up is actually closer to 0.24%, so it does include some plutonium. The control rod chosen is ID L42295 with a burnup of 0.258%. A blanket sub-assembly was also chosen as the basis for the blanket region, and its position within the core was 11D04. The positions for C2893E and L42295 are shown in Figure 6.



MCNP also calculates the Shannon entropy of the system in regards to the fission source distribution. Shannon entropy is “a well-known concept from information theory and provides a single number for each batch to help characterize convergence of the fission source distribution.”<sup>(10)</sup> Shannon entropy will converge to a single value as the distribution of the source becomes stationary. This means that, for MCNP calculations, a single generation can be identified that marks the place where the fission source has converged for the system.

If the calculation of the criticality of the system includes the generations which are below the Shannon entropy value, erroneous data is included since the fission source has not yet converged. This means that the calculations from generations below the Shannon entropy value must be discarded before the criticality of the system can be calculated. MCNP has tools that assist in deciding the number of generations that must be discarded in order to give the system time to properly distribute the fission source.

The materials that are created within MCNP can include any number of isotopes at different atomic or weight densities. Because the nature of neutron collision is dependent on the energy of the neutron, each isotope must be given a spectrum of collision probabilities.

The cross-section of an isotope is dependent on both the speed that the neutron is travelling, and the speed that the target nuclei are travelling. This difference in the relative speed of the neutron is what gives rise to the “Doppler shift” effect in resonance cross-section behavior<sup>(11)</sup>. Figure 7 shows the qualitative result of Doppler broadening.

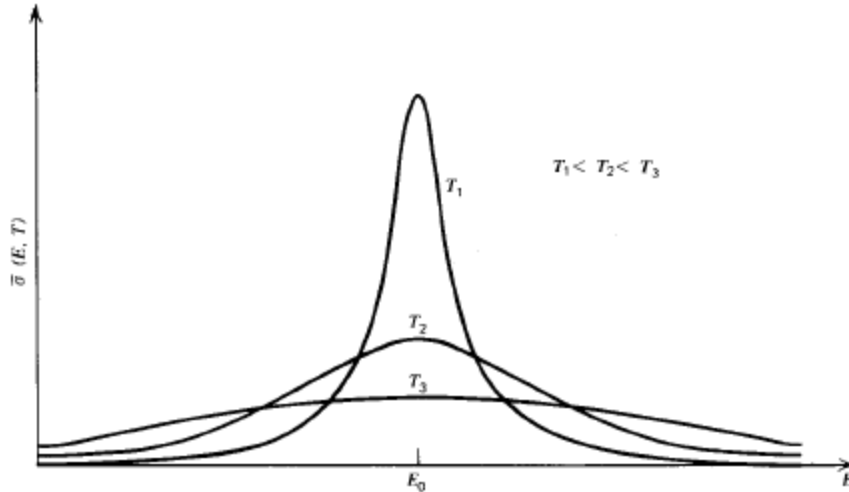


Figure 7. Example of Doppler Broadening.

For example, imagine that for some isotope, the cross-section, dependent on energy and temperature, were equal to 1 barn. For simplicity, the  $\Gamma$  value will be equal to 0.001, and the  $\Gamma_\gamma$  value will be one tenth of that, at 0.0001. An assumption will also be made that the energy of the neutron that is interacting with the isotope is thermal ( $\sim 0.0253\text{eV}$ ), and does not change in this contrived example. If the assumed isotope is the same size as hydrogen ( $A=1$ ), and temperature changes by  $100^\circ\text{C}$ , the  $\Gamma_D$  value becomes 0.0096. This means the value of  $x$  would be 0, and the value of  $\zeta$  would be 0.10. Using Table 2-2 of Duderstadt<sup>(11)</sup>, the value of the  $\Psi(\zeta, x)$  function becomes 0.08384. Using these values, a new cross-section can be calculated for the new temperature, equal to 0.8384 barns.

While the Doppler broadening is important, the other important factor is the energy of the neutrons that are incident on the isotopes that have been broadened. Even though the cross-sections have been shifted to account for slightly higher or slightly lower energy neutrons, there still has to be enough neutrons in that new energy range to interact with the

new cross-sections. The energy flux spectrum of EBR-II is shown in Figure 8, where the flux values are normalized to the maximum per source particle flux of  $1.64\text{E-}04 \text{ n/cm}^2$ .

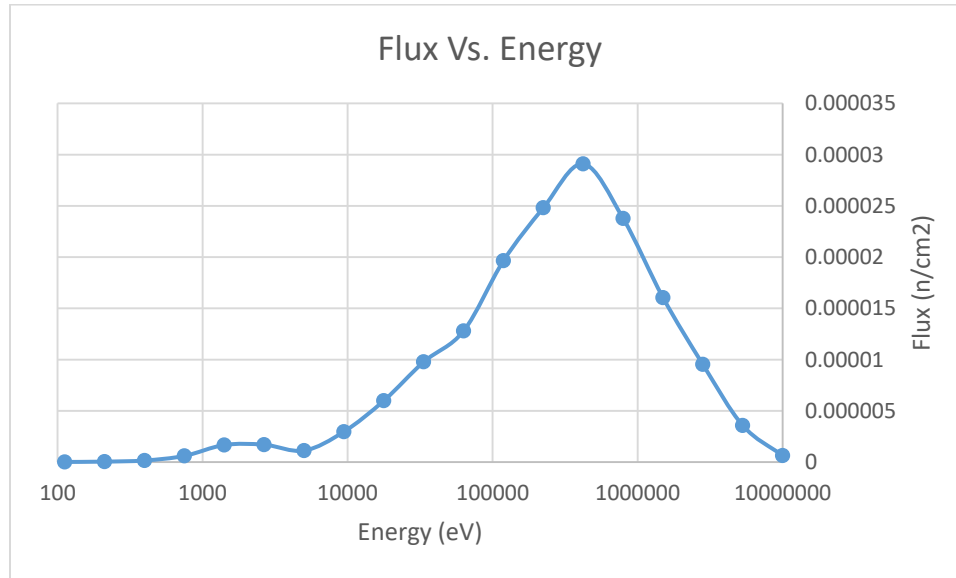


Figure 8. Energy Flux Spectrum of EBR-II

This plot shows comparatively very few neutrons in the epithermal energy region (between  $1\text{E}03$  and  $1\text{E}04$ ) that will be affected by the change in the cross-sections. Most of the neutrons in the core will be unaffected, since they have an energy that was within the range of the original cross-sections.

To correct for the Doppler effect, NJOY was used to change the cross-sections depending on the temperature. It performed the Doppler broadening at a variety of energies for the given temperature. NJOY was used to calculate new cross-sections at various temperatures across the gradient.

Using MCNP and NJOY, a model was created that included all of the relevant materials and geometries for the EBR-II Run 138B core, as well as changes the cross-sections of materials to reflect different temperature regions within the core. If each

temperature region is appropriately chosen, the model should reflect the real behavior of sodium, which is that the innermost assembly of the core should be the hottest, while the outermost assembly should be the coolest.

For this simplified model, many of the regions of the core were homogenized. To ensure these areas are accurately homogenized, as well as to ensure these areas are capable of being homogenized, some precautions have to be taken. The six factor formula (Equation 7) will be used to describe some of the qualities of heterogeneous and homogeneous models.

$$k = \varepsilon \eta f p P_{NLTh} P_{NLf} \quad \text{Equation 7}^{(11)}$$

where k = multiplication factor

$$\varepsilon = \text{fast fission factor} = \frac{\text{total number of fission neutrons}}{\text{number of fission neutrons from thermal fissions}}$$

$$\eta = \text{thermal fission factor} = \frac{\sigma_f^{Fuel}}{\sigma_a^{Fuel}}$$

p=resonance escape probability = fraction of fission neutrons that manage to slow down from fission to thermal energies

$$f = \text{thermal utilization factor} = \frac{\text{number of thermal neutron absorptions in fuel}}{\text{total number of thermal neutron absorptions}}$$

$P_{NL\text{-thermal}}$  = probability of non-leakage of thermal neutrons

$P_{NL\text{-fast}}$  = probability of non-leakage of fast neutrons

It is important to note that the six-factor formula deals mostly with thermal reactors, but it is relevant to discuss in EBR-II. In a heterogeneous thermal reactor, fuel lumping increases the value of  $k$ . This is because the fuel is subject to self-shielding, which raises the value of  $p$ , since the fuel aids in slowing down fast neutrons into the thermal region. In addition to the increase in  $p$ ,  $f$  actually suffers a non-negligible decrease, due to a depressed thermal flux in the fuel. However, the important thing to note is that  $\epsilon$  also increases as a result of lumped fuel, since a newly born fission neutron will have a higher chance of interacting with fuel material<sup>(11)</sup>.

These are all important factors to keep in mind when comparing a homogenous core and a heterogeneous one for thermal reactors. However, EBR-II has an interesting characteristic which is its sodium coolant. Normally, a fast reactor would not be subject to these kinds of heterogeneous phenomena, and in fact would not suffer much from being homogenized. In EBR-II, the sodium coolant acts as a reflector for neutrons that escape from fuel pins. This is important because sodium scattering events increase the reactivity of the core, by reflecting neutrons back into fuel. If the amount of sodium is effectively reduced by reducing its density, the reactivity of the system will decrease, since more neutrons will escape. This also means that homogenization of the core will increase reactivity, as more fuel atoms will be near sodium atoms, which will increase the rate that neutrons are reflected back to fuel atoms in order to cause fissions.

Often it is easiest to homogenize a large core by taking a small unit cell and homogenizing it first. After a small unit cell is acquired, volume fractions are used to “smear” it across a larger volume. As long as the number of atoms are conserved, this

approach is viable. For the simplified model, one sub-assembly's core region will be homogenized and scaled up to the full size of the core region by volume fractions.

Since this is a simple model, each sub-assembly is not modeled individually. Instead, an average of all the materials within a hexagonal region of the core are used, and radially increasing hexagonal prisms represent "rings" of temperature within the core. Axial divisions of the fuel region are also incorporated.

The hexagonal reactor simple model is assumed to have a flux shape that follows a right circular cylinder. This means that the flux shape in the radial direction follows a Bessel function of order zero, and the flux shape in the axial direction follows a cosine function<sup>(11)</sup>. The flux profile shape for EBR-II is shown in Figure 9.

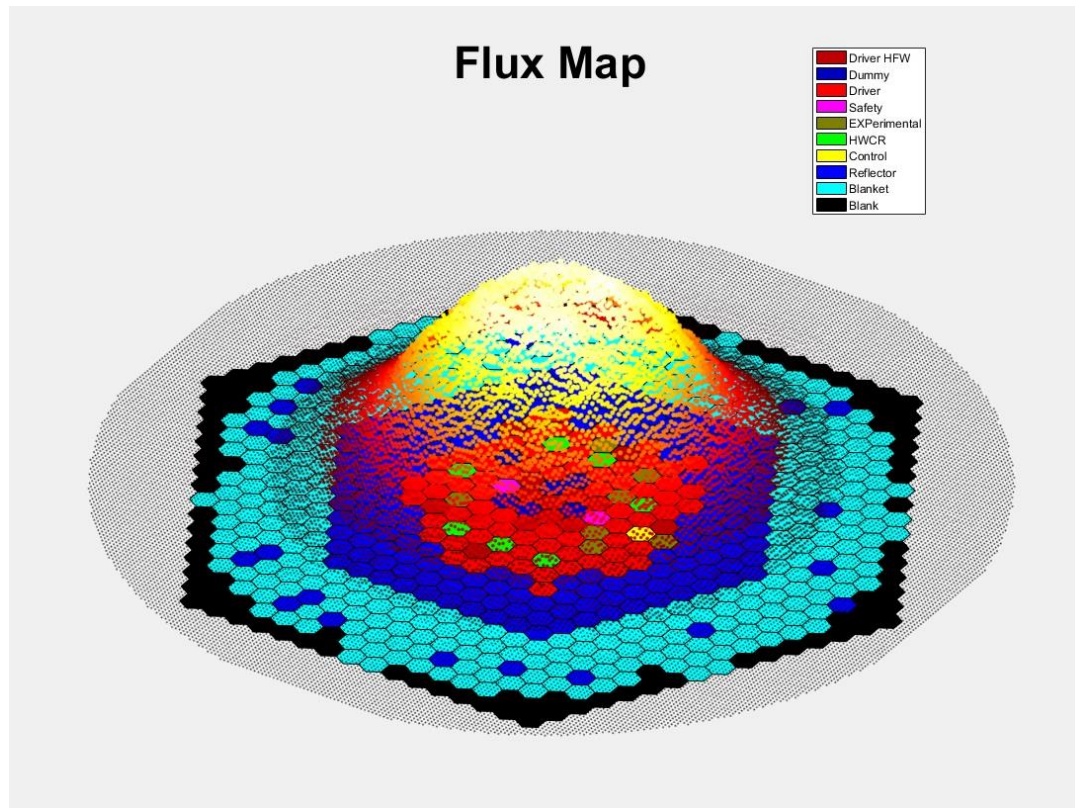


Figure 9. Flux Map of EBR-II<sup>(C)</sup>.

## Modeling

A simplified model was created for the EBR-II core, as a simple model made it easier to manipulate the sodium temperatures to create a sodium temperature gradient.

The simplified model included all fissile material in the core, as well as sodium for the coolant and stainless steel. These materials were homogenized into three distinct regions: the inner core, the stainless steel reflector, and the outer blanket. Each of these regions were divided axially to include upper and lower extension regions, also homogenized. The upper and lower extensions for the lower extension for the inner core were modeled as a 51.6% sodium 48.4% stainless steel 304 mixture. The upper extension

---

<sup>C</sup> Picture generated using MICKA.

for the inner core has a 51.6/48.4 smear, but also includes B<sub>4</sub>C, which is found in high worth control rod upper extensions. The stainless steel dummy sections have a 90/10 mixture of stainless steel to sodium ratio. There was an argon plenum gas region above the inner core region.

The simplified model can be seen in Figure 10 and Figure 11. Figure 10 shows the plan view where blue is the outer blanket, green is the stainless steel reflector, and purple is the inner core. Figure 11 shows the elevation view of the model, where yellow is the upper and lower extensions, dark blue is the B<sub>4</sub>C added upper extension, and orange is the plenum gas region.

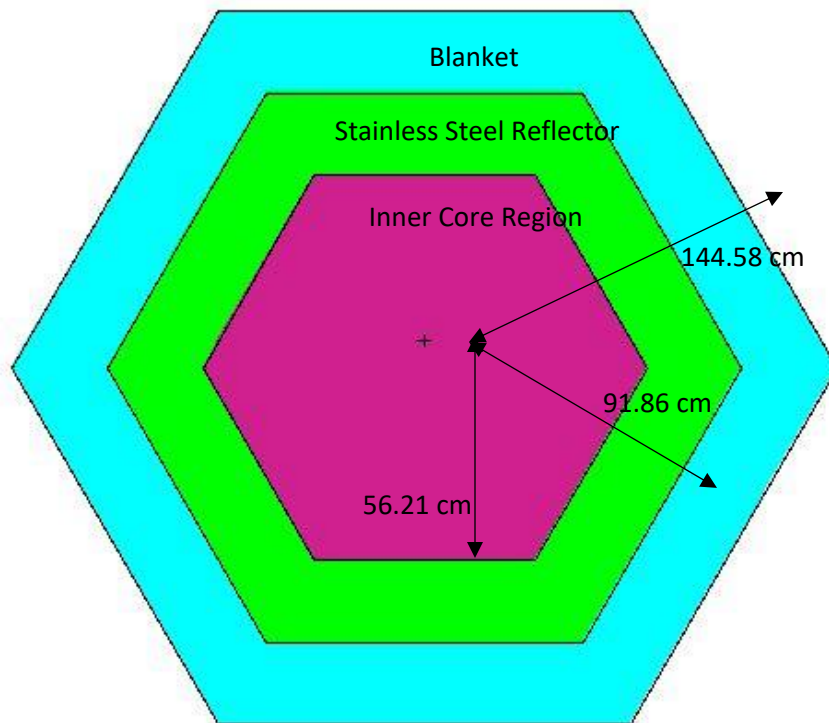


Figure 10. Plan View of Simplified Model.

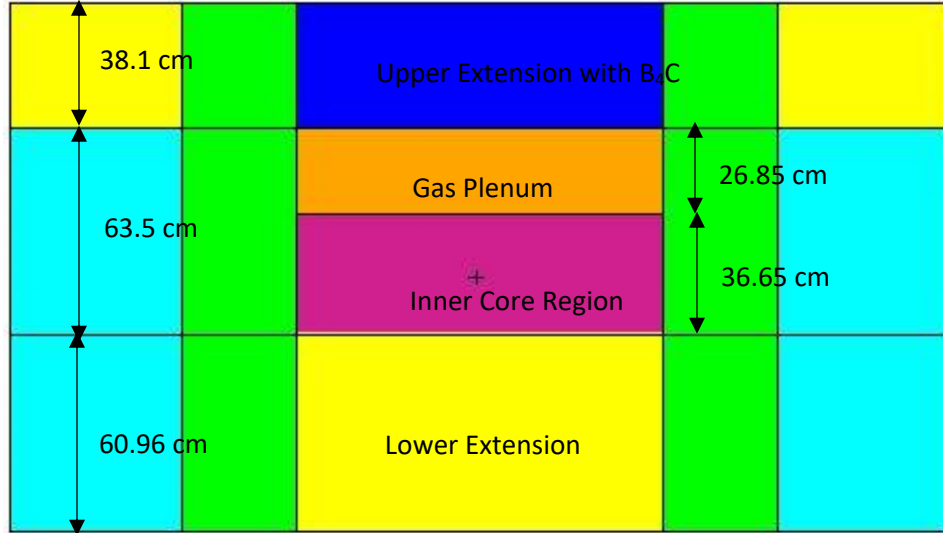


Figure 11. Elevation View of Simplified Model.

The middle prism of the inner core was divided into smaller prisms, each made up of stainless steel, sodium, U<sup>235</sup>, U<sup>238</sup>, Pu<sup>239</sup>, Pu<sup>240</sup>, and Pu<sup>241</sup>. The sodium of these regions have different densities, which represent different temperatures, and their collision spectra were manipulated using NJOY. The innermost prism was the hottest, and each prism moving both axially and radially out were cooler.

## Dimensions

A single sub-assembly pitch was equal to 5.89 cm. Using the active height of the core's fuel, which is 36.65 cm<sup>3</sup>, the volume of a sub-assembly was calculated using Equation 8,

$$V = P^2 \frac{\sqrt{3}}{2} h \quad \text{Equation 8}$$

where  $P$  is the pitch of the sub-assembly, and  $h$  is the height.

The volume of a single sub-assembly middle region was equal to 1102.17cm<sup>3</sup>. Using the number of sub-assemblies for each region and multiplying it by the volume of a single sub-assembly gave the volume of the total region. This volume was then used to calculate the pitch of the region for the model.

The number of sub-assemblies within each region and its corresponding pitch conversion for the model are shown in Table 2. Note that the number of sub-assemblies does not refer to the number of a type of sub-assembly, but simply the combined sub-assembly volume.

Table 2. Dimensions of Simplified Model.

Dimensions (cm)	Number of Sub-assemblies	Pitch (cm)
Inner Core	91	56.21
Stainless Steel Reflector	243	91.86
Outer Blanket	602	144.58

The heights of each region in the sub-assemblies can vary based on the type of sub-assembly, and were normalized for the simple model. The height of the lower extension was 60.96 cm and the height of the upper extension was 38.1 cm. The height of the middle section for the core region is 36.65 cm with a plenum region of 26.86 cm. The height of the middle section for the stainless steel and blanket was 63.5 cm.

## Materials

The Neutronics Benchmark Specifications for EBR-II Shutdown Heat Removal Test SHRT-45R – Revision 1<sup>(6)</sup> gave guidance for the volume ratios of each material for

each fueled region of the core. It also gave the atom densities of the fueled regions of each sub-assembly in the core. Table 3 shows the volume ratios used in the simplified model.

Table 3. Volume Fractions for Materials.

Core Composition by Volume %	Fuel	Stainless Steel	Sodium
Driver	0.2692	0.2229	0.5079
Control Rod	0.1804	0.2269	0.5927
Blanket	0.611	0.176	0.212

The model used sodium at various temperatures for the temperature gradient across the core. The highest sub-assembly temperature and bulk sodium temperature comes from the EBR-II Logbook during Run-138B<sup>(13)</sup>. The sodium densities were calculated using Equation 9<sup>(4)</sup>.

$$\rho_l = \rho_c + f \left(1 - \frac{T}{T_c}\right) + g \left(1 - \frac{T}{T_c}\right)^h \quad \text{Equation 9}$$

for  $371 \text{ K} \leq T \leq 2503.7$ , where

$$\rho_c = 219 \text{ kg/m}^3$$

$$f = 275.32$$

$$g = 511.58$$

$$h = 0.5$$

$$T_c = 2503.7 \text{ K}$$

The sodium temperatures and their corresponding densities are shown in Table 4.

Table 4. Sodium Density at Different Temperatures.

Temperature (°C)	Density (g/cm <sup>3</sup> )
------------------	------------------------------

358.89	0.8671
363.44	0.8661
365.19	0.8657
365.32	0.8657
365.83	0.8656
366.05	0.8655
367.06	0.8653
367.7	0.8651
367.8	0.8651
368.44	0.865
388.29	0.8604
399.58	0.8578
400.38	0.8576
403.71	0.8569
405.14	0.8566
411.67	0.8551
415.8	0.8541
416.43	0.854
420.56	0.853

The model required the atom fractions of all of the isotopes for a certain region of the core, as well as the total atom density of the region. The atom fractions and total atom density for each region of the core can be found in Tables 5 through Table 9.

Table 5. Material Data for Inner Core.

<b>Inner Core</b>	
Isotope	Atom Fraction
Uranium-234	1.1552E-08
Uranium-235	9.3049E-03
Uranium-236	1.2720E-06
Uranium-238	4.5880E-03
Plutonium-236	4.2386E-16
Plutonium-238	1.4635E-12
Plutonium-239	3.5685E-07
Plutonium-240	1.7069E-11
Plutonium-241	7.1396E-16
Plutonium-242	2.0265E-20
Carbon-12	5.3689E-04

Silicon-28	1.5126E-03
Silicon-29	7.6804E-05
Silicon-30	5.0630E-05
Phosphorus-31	3.2715E-05
Sulfur-32	1.6363E-05
Sulfur-33	1.3100E-07
Sulfur-34	7.3946E-07
Sulfur-36	3.4474E-09
Chromium-50	1.4357E-03
Chromium-52	2.7685E-02
Chromium-53	3.1393E-03
Chromium-54	7.8143E-04
Manganese-55	1.2744E-03
Iron-54	6.8507E-03
Iron-56	1.0754E-01
Iron-57	2.4836E-03
Iron-58	3.3052E-04
Nickel-58	9.5629E-03
Nickel-60	3.6836E-03
Nickel-61	1.6007E-04
Nickel-62	5.1054E-04
Nickel-64	1.3002E-04
Sodium-23	1.0327E-01

Note that the inner core region numbers change as the sodium density changes, and the above numbers are only for sodium at 420.56°C. The inner core numbers for each temperature are shown in Appendix A.

Table 6. Material Data for Blanket Region.

<b>Blanket</b>	
Isotope	Atom Fraction
Uranium-234	6.7029E-10
Uranium-235	5.6084E-04
Uranium-236	4.4201E-06
Uranium-238	2.7011E-01
Plutonium-236	3.0537E-14
Plutonium-238	9.7501E-09
Plutonium-239	2.0959E-03
Plutonium-240	1.5117E-05
Plutonium-241	1.4314E-07

Plutonium-242	4.0564E-10
Carbon-12	2.4738E-04
Silicon-28	6.9695E-04
Silicon-29	3.5389E-05
Silicon-30	2.3329E-05
Phosphorus-31	1.5074E-05
Sulfur-32	7.5396E-06
Sulfur-33	6.0361E-08
Sulfur-34	3.4072E-07
Sulfur-36	1.5885E-09
Chromium-50	6.6151E-04
Chromium-52	1.2757E-02
Chromium-53	1.4465E-03
Chromium-54	3.6006E-04
Manganese-55	5.8719E-04
Iron-54	3.1566E-03
Iron-56	4.9552E-02
Iron-57	1.1444E-03
Iron-58	1.5230E-04
Nickel-58	4.4063E-03
Nickel-60	1.6973E-03
Nickel-61	7.3756E-05
Nickel-62	2.3525E-04
Nickel-64	5.9910E-05
Sodium-23	2.4511E-02

Table 7. Material Data for Stainless Steel Reflector.

<b>Stainless Steel Reflector</b>	
Isotope	Atom Fraction
Carbon-12	2.2793E-03
Silicon-28	6.4214E-03
Silicon-29	3.2606E-04
Silicon-30	2.1494E-04
Phosphorus-31	1.3889E-04
Sulfur-32	6.9467E-05
Sulfur-33	5.5614E-07
Sulfur-34	3.1393E-06
Sulfur-36	1.4635E-08
Chromium-50	6.0949E-03
Chromium-52	1.1753E-01
Chromium-53	1.3327E-02
Chromium-54	3.3175E-03
Manganese-55	5.4101E-03

Iron-54	2.9084E-02
Iron-56	4.5655E-01
Iron-57	1.0544E-02
Iron-58	1.4032E-03
Nickel-58	4.0598E-02
Nickel-60	1.5638E-02
Nickel-61	6.7956E-04
Nickel-62	2.1674E-03
Nickel-64	5.5198E-04
Sodium-23	2.0849E-02

Table 8. Material Data for Upper and Lower Extensions.

<b>Upper and Lower Extensions</b>	
Isotope	Atom Fraction
Carbon-12	1.2663E-03
Silicon-28	3.5674E-03
Silicon-29	1.8115E-04
Silicon-30	1.1941E-04
Phosphorus-31	7.7160E-05
Sulfur-32	3.8593E-05
Sulfur-33	3.0897E-07
Sulfur-34	1.7440E-06
Sulfur-36	8.1308E-09
Chromium-50	3.3860E-03
Chromium-52	6.5297E-02
Chromium-53	7.4041E-03
Chromium-54	1.8430E-03
Manganese-55	3.0056E-03
Iron-54	1.6158E-02
Iron-56	2.5364E-01
Iron-57	5.8576E-03

Iron-58	7.7955E-04
Nickel-58	2.2554E-02
Nickel-60	8.6879E-03
Nickel-61	3.7753E-04
Nickel-62	1.2041E-03
Nickel-64	3.0666E-04
Sodium-23	1.0425E-01

Table 9. Material Data for Upper Extension Inner Core.

<b>Upper Extension Including B<sub>4</sub>C</b>	
Isotope	Atom Fraction
Carbon-12	4.8379E-02
Silicon-28	6.1373E-04
Silicon-29	3.1164E-05
Silicon-30	2.0543E-05
Phosphorus-31	1.3274E-05
Sulfur-32	6.6394E-06
Sulfur-33	5.3154E-08
Sulfur-34	3.0004E-07
Sulfur-36	1.3988E-09
Chromium-50	5.8253E-04
Chromium-52	1.1233E-02
Chromium-53	1.2738E-03
Chromium-54	3.1707E-04
Manganese-55	5.1708E-04
Iron-54	2.7797E-03
Iron-56	4.3636E-02
Iron-57	1.0077E-03

Iron-58	1.3411E-04
Nickel-58	3.8802E-03
Nickel-60	1.4946E-03
Nickel-61	6.4950E-05
Nickel-62	2.0716E-04
Nickel-64	5.2757E-05
Sodium-23	1.6698E-02
Boron-10	5.7770E-02
Boron-11	5.2542E-02

It is important to show that the other materials within the inner core were not losing or gaining any atoms due to the sodium density changes. Table 10 shows the atom density of both sodium and  $^{235}\text{U}$  for each temperature.

Table 10. Atom Densities of Sodium and  $^{235}\text{U}$ .

Temperature (°C)	Atom Density of Sodium (atm/b/cm)	Atom of Density of $^{235}\text{U}$ (atm/b/cm)
358.89	1.1890E-02	1.0713E-03
363.44	1.2072E-02	1.0713E-03
365.19	1.2067E-02	1.0713E-03
365.32	1.2066E-02	1.0713E-03
365.83	1.2065E-02	1.0713E-03
366.05	1.2064E-02	1.0713E-03
367.06	1.2061E-02	1.0713E-03
367.7	1.2059E-02	1.0713E-03
367.8	1.2058E-02	1.0713E-03
368.44	1.2056E-02	1.0713E-03
388.29	1.1993E-02	1.0713E-03
399.58	1.1957E-02	1.0713E-03
400.38	1.1954E-02	1.0713E-03
403.71	1.1944E-02	1.0713E-03
405.14	1.1939E-02	1.0713E-03
411.67	1.1918E-02	1.0713E-03

415.8	1.1905E-02	1.0713E-03
416.43	1.1903E-02	1.0713E-03
420.56	1.1890E-02	1.0713E-03

The atom density of  $^{235}\text{U}$  is unchanged, but in Appendix A, the atom fraction of  $^{235}\text{U}$ , as well as all the atom fractions of the other isotopes involved in the core region material, change as sodium density changes.

## Gradient

The inner core fuel region was discretized equally into five axial planes and three hexagonal prisms, making up 25 discrete regions within the inner core. Figure 12 shows the model with the discretized regions.

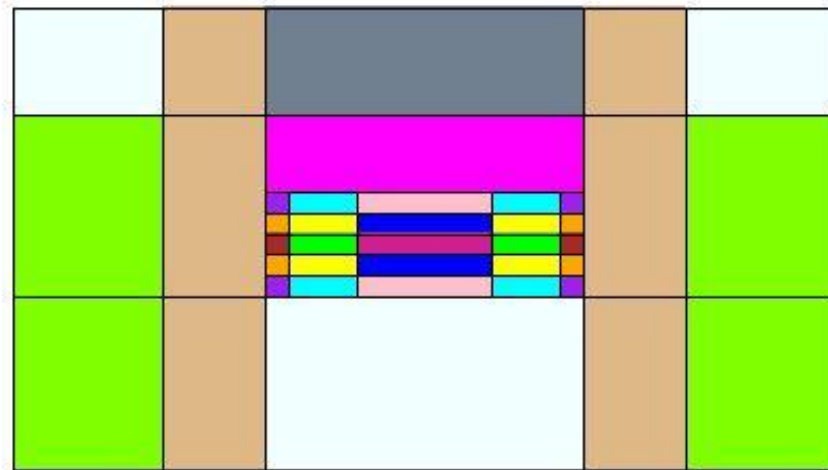


Figure 12. Side View of Simplified Model with Gradient.

The gradient was calculated by taking a combination of a Bessel function of order zero in the radial direction, and a cosine in the axial direction, and applying that to the change in temperature from the highest temperature in the center assembly to bulk temperature at the bounds. Two gradients were actually created in order to find the difference between changes in temperature. The first gradient is from bulk sodium

temperature to the highest recorded temperature, and the second gradient is from the lowest temperature up to the temperature that corresponds with the reactor at a low power. The reason for this is that a gradient require two temperature bounds, and there needed to be a large enough change in temperature between these two models to get an accurate change in reactivity. Figures 13 through 16 show the axial and radial temperature numbers and positions for the gradient that runs from 358°C to 420°C, and for the gradient that runs from 358°C to 368°C.

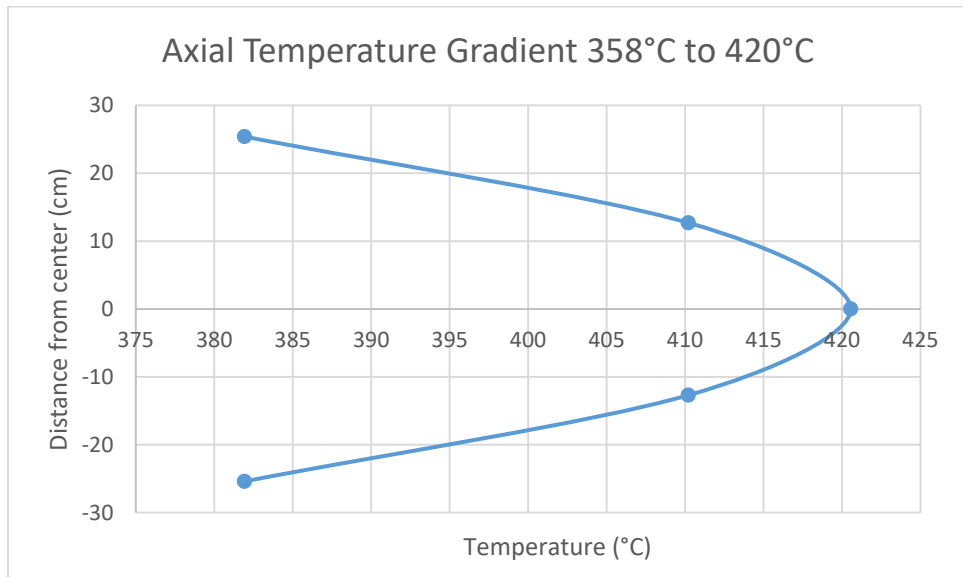


Figure 13. Axial Temperature Gradient 358°C to 420°C.

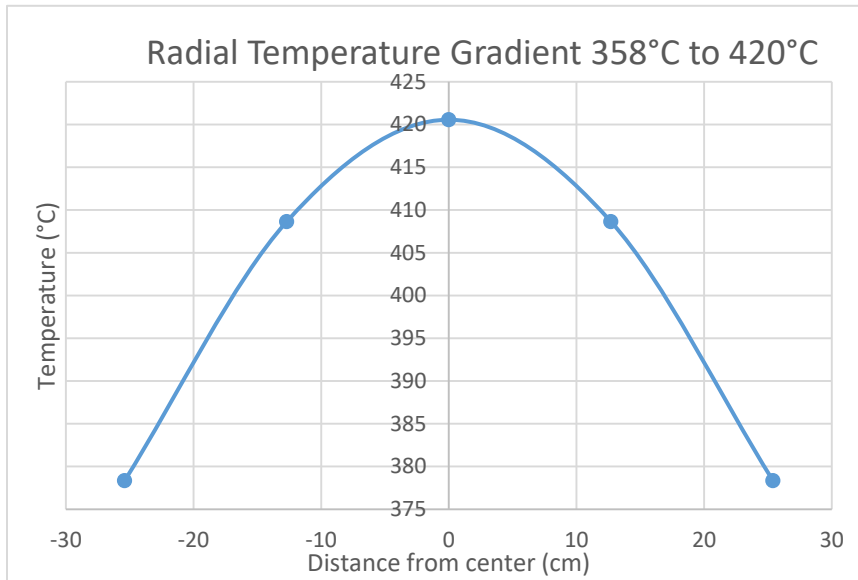


Figure 14. Radial Temperature Gradient 358°C to 420°C.

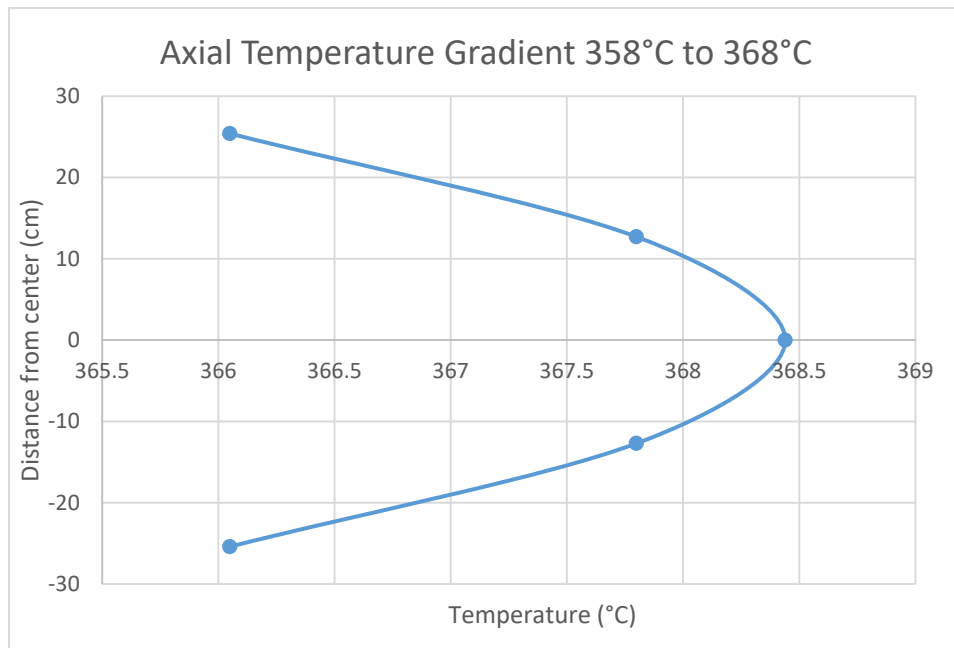


Figure 15. Axial Temperature Gradient 358°C to 368°C.

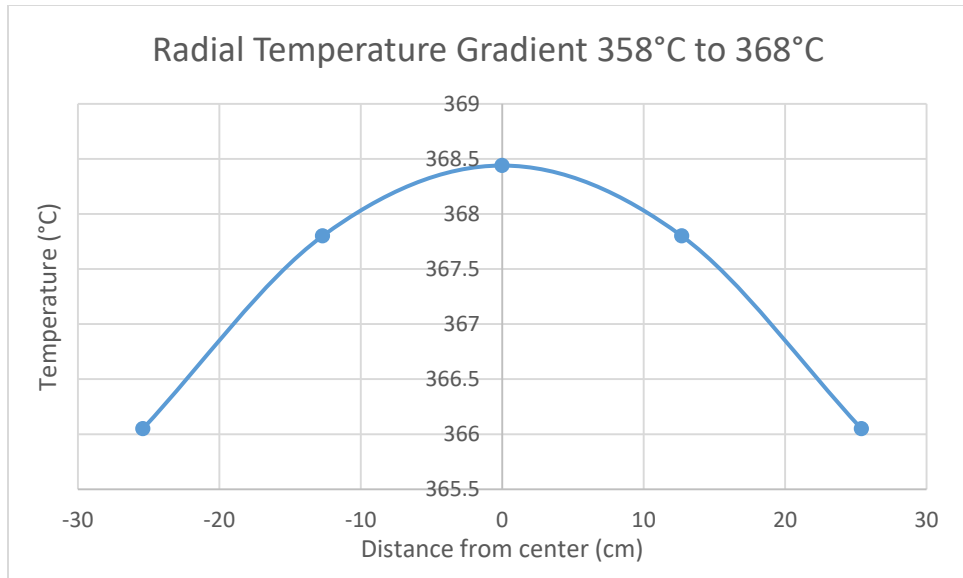


Figure 16. Radial Temperature Gradient 358°C to 368°C.

The temperatures in °C and their corresponding positions for the gradient that runs from 358°C to 420°C are shown in Figure 17.

380.13	395.28	381.93	395.28	380.13
394.27	409.42	410.21	409.42	394.27
378.34	408.64	420.56	408.64	378.34
394.27	409.42	410.21	409.42	394.27
380.13	395.28	381.93	395.28	380.13

Figure 17. Gradient Temperatures from 358°C to 420°C.

Figure 18 shows the positions and temperatures in °C for the gradient model that runs from 358°C to 368°C.

363.44	365.32	366.05	365.32	363.44
365.19	367.06	367.80	367.06	365.19
365.83	367.70	368.44	367.70	365.83
365.19	367.06	367.80	367.06	365.19
363.44	365.32	366.05	365.32	363.44

Figure 18. Gradient Temperatures from 358°C to 368°C.

NJOY was used to create a new cross-section library that has the adjusted higher temperature cross-sections for all the materials in the core. Figure 19 shows the difference between the U-238 cross-section at room temperature (23°C) and at 2,226°C for the 10eV

peak. The 10 eV peak is shown only because it is a distinct resonance for U-238. While the model does not reach this high of temperatures, the Doppler broadening is more apparent over this large temperature change.

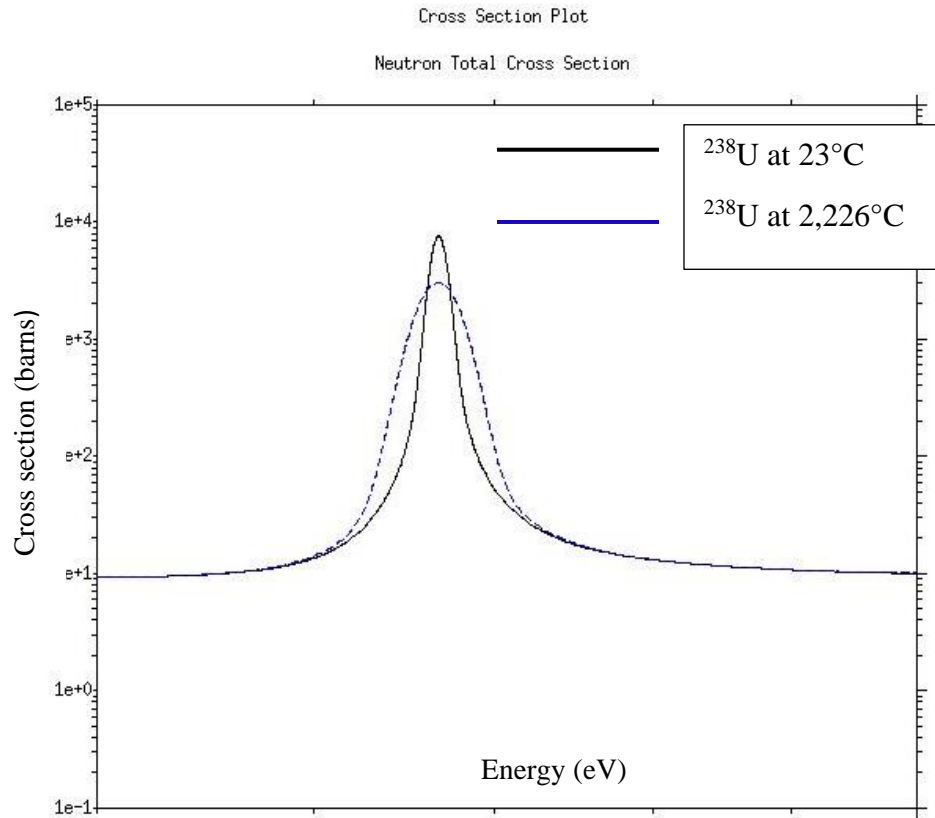


Figure 19.  $^{238}\text{U}$  Cross-Section at 23°C vs.  $^{238}\text{U}$  Cross-Section at 2,226°C near 10eV

## Results

Each model was run with 100,000 neutrons per generation, and 1,000 generations. The first 200 generations were discarded to reach a uniform fission distribution, which occurred at 190 generations for this model, according to MCNP. Four models in total were run to determine the effect of changing sodium density across the core. These four models used sodium at different temperatures as determined from the EBR-II Logbook<sup>(13)</sup>. 358°C

corresponds to the temperature of the core when just the sodium heaters are running, while 420°C corresponds to the core at full power. 368° was the temperature that corresponded to the core when it was at a power of 20 MW. The first two models were created with all sodium in the inner core region at one temperature. The two temperatures were nominally 358°C and 420°C. The last two models created were gradient models that had two different high temperatures. The low-end of both gradient models was 358°C, but the high ends were nominally 368°C and 420°C. The results of each of these runs appear in Table 11.

Table 11. Calculated Model Results.

Model Results	$k_{\text{eff}}$
Bulk at 358	1.0565 ± 0.00008
Bulk at 420	1.0558 ± 0.00008
Gradient at 368	1.0456 ± 0.00008
Gradient at 420	1.0452 ± 0.00009

A Study of the Temperature Coefficients of Reactivity for EBR-II Run 93<sup>(5)</sup> gives the temperature coefficients for different changes in EBR-II. For sodium density, the coefficient is  $-7.98\text{E-}06 \Delta k/^\circ\text{C}$ . For Doppler broadening, the coefficient is given by Equation 10.

$$\frac{\partial k}{\partial T} = \frac{-3.6650\text{E-}4}{T+273} \Delta k/^\circ\text{C} \quad \text{Equation 10}$$

where T is in °C.

For the bulk models, the change in temperature was 61.67°C, and for the gradient models, the change in temperature was 52°C. The discrepancy between these temperature changes is due to how the gradient is calculated. The bulk-to-bulk models used only one

temperature each, so the highest and lowest temperature available are used. However, to create a temperature gradient, two temperatures are needed for each model. Both models used the same low temperature, but the change in temperature was measured from the hottest temperature, which was slightly higher in the second gradient model as compared to the low temperature bulk model. This was also why the expected  $\Delta k$  for each of these runs are different, as the reactivity coefficient for sodium temperature was being calculated for two different temperature changes. Table 12 shows the calculated reactivity change for each run and the percent difference from the projected value.

Table 12. Calculated Results.

Calculated Reactivity Change	Model $\Delta k$	Expected $\Delta k$	Percent Difference
Bulk-to-Bulk	-7.00E-04	-4.92E-04	42.24%
Gradient-to-Gradient	-4.00E-04	-4.15E-04	4%

While the results for the model  $\Delta k$  might seem strange, this is because the change is only happening in the 4<sup>th</sup> decimal place. MCNP only reports to the 4<sup>th</sup> decimal place, which makes the  $\Delta k$  seem more precise. This can be seen by taking the difference between the gradient runs, 1.0456 subtracted by 1.0452, which is 4E-04 exactly.

A calculation was performed that changed the cross-section data in conjunction with the sodium density. The cross-section of sodium was changed as the temperature increased, so that both the cross-section data and the density were representative of the temperature in that region of the core. This calculation results in an error of 36%, which is large compared to the gradient-to-gradient comparison, especially when these models are almost identical except for the use of NJOY. This is indicative of an issue with small

temperature adjustments in NJOY. When the cross-sections were adjusted to the bulk sodium temperature, the  $\Delta T$  is nominally 335°C. However, the  $\Delta T$  between each gradient section is only on the order of 10°C, and the overall  $\Delta T$  of the gradient is 62°C. It is possible that such small temperature changes relate to a too large broadening of the cross-section, since the change from the expected value is so large. This also shows the issue that there are not enough neutrons with energies affected by the change in cross-sections due to Doppler broadening. There are too few interactions at that energy to have much of an impact, even with broadened cross-sections. These results are included in Appendix B.

## Conclusion

The calculated sodium temperature coefficient of reactivity, using a gradient assumption, was  $-7.69\text{E-}06 \Delta k/^{\circ}\text{C}$ . This compares well with the published result of  $-7.98\text{E-}06 \Delta k/^{\circ}\text{C}$ . The assumption of bulk sodium temperature in the core is not suitable for the EBR-II model. The bulk-to-bulk model gives a 42% difference from the expected value, which shows that it cannot be assumed that the sodium throughout the inner core is at the same temperature. A gradient must be used to accurately represent the conduction of heat from the center of the core moving away both axially and radially. This means that any modelling of the EBR-II inner core region must include a sodium density gradient to properly model the core. If a gradient cannot be applied to the core, for instance, in a large detailed model, the temperature coefficient gives a good representation of the sodium density change within the core.

## References

- 1) *MCNP – A General Monte Carlo N-Particle Transport Code, Version 5, Volume I: Overview and Theory*, X-5 Monte Carlo Team, April 24, 2003.
- 2) *The NJOY Nuclear Data Processing System, Volume I: User's Manual*, R. E. MacFarlane, D. W. Muir, R. M. Boicourt, May, 1982.
- 3) *Evaluation of Neutron Nuclear Data for Sodium-23*, Keiichi Shibata, 07 February 2012.
- 4) *Thermodynamic and Transport Properties of Sodium Liquid and Vapor*, J. K. Fink, and L. Leibowitz, January 1995.
- 5) *A Study of the Temperature Coefficients of Reactivity for EBR-II Run 93*, M.L. Carboneau, H. A. Larson, E. M. Dean, and V. P. Charyulu, November 1980.
- 6) *Neutronics Benchmark Specifications for EBR-II Shutdown Heat Removal Test SHRT-45R – Revision 1*, T. Fei, A. Mohamed, and T. K. Kim, January 23, 2013.
- 7) *EBR-II System Design Descriptions: Volume II Primary System: Chapter 2 Reactor*, F.E. Metcalf, J. T. Natoce, W. A. Rupp, F. J. Tebo, and E. Hutter, February 15, 1985.
- 8) *Introduction to Nuclear Engineering, Third Edition*, John R. Lamarsh, and Anthony J. Baratta, 2001.
- 9) *Spent Nuclear Fuel Assembly Inspection Using Neutron Computed Tomography*, Pope C. L., December 2010.
- 10) *On the Use of Shannon Entropy of the Fission Distribution for Assessing Convergence of Monte Carlo Criticality Calculations*, Forrest B. Brown, September 2006.
- 11) *Nuclear Reactor Analysis*, James J. Duderstadt, Louis J. Hamilton, 1976.

12) *Cross-Section Table*, Japan Atomic Energy Agency, Nuclear Data Center, 2016.

13) *Experimental Breeder Reactor II Console Log Book Volume 392*, 1986.

## Appendix

### A. Additional Material Data for Inner Core

Atom Fraction for Inner Core for Corresponding Temperatures (°C)						
Isotope	420.56	416.43	415.8	411.67	405.14	403.71
Uranium-234	1.1552E-08	1.1550E-08	1.1549E-08	1.1547E-08	1.1543E-08	1.1542E-08
Uranium-235	9.3049E-03	9.3029E-03	9.3026E-03	9.3006E-03	9.2974E-03	9.2967E-03
Uranium-236	1.2720E-06	1.2717E-06	1.2716E-06	1.2714E-06	1.2709E-06	1.2708E-06
Uranium-238	4.5880E-03	4.5870E-03	4.5869E-03	4.5859E-03	4.5843E-03	4.5840E-03
Plutonium-236	4.2386E-16	4.2377E-16	4.2375E-16	4.2366E-16	4.2352E-16	4.2349E-16
Plutonium-238	1.4635E-12	1.4632E-12	1.4631E-12	1.4628E-12	1.4623E-12	1.4622E-12
Plutonium-239	3.5685E-07	3.5677E-07	3.5676E-07	3.5668E-07	3.5656E-07	3.5653E-07
Plutonium-240	1.7069E-11	1.7065E-11	1.7064E-11	1.7061E-11	1.7055E-11	1.7054E-11
Plutonium-241	7.1396E-16	7.1381E-16	7.1379E-16	7.1363E-16	7.1339E-16	7.1333E-16
Plutonium-242	2.0265E-20	2.0260E-20	2.0260E-20	2.0255E-20	2.0248E-20	2.0247E-20
Carbon-12	5.3689E-04	5.3677E-04	5.3675E-04	5.3664E-04	5.3645E-04	5.3641E-04
Silicon-28	1.5126E-03	1.5122E-03	1.5122E-03	1.5119E-03	1.5113E-03	1.5112E-03
Silicon-29	7.6804E-05	7.6788E-05	7.6785E-05	7.6768E-05	7.6742E-05	7.6737E-05
Silicon-30	5.0630E-05	5.0619E-05	5.0617E-05	5.0606E-05	5.0589E-05	5.0585E-05
Phosphorus-31	3.2715E-05	3.2708E-05	3.2707E-05	3.2700E-05	3.2689E-05	3.2687E-05
Sulfur-32	1.6363E-05	1.6359E-05	1.6359E-05	1.6355E-05	1.6350E-05	1.6349E-05
Sulfur-33	1.3100E-07	1.3097E-07	1.3097E-07	1.3094E-07	1.3089E-07	1.3088E-07
Sulfur-34	7.3946E-07	7.3930E-07	7.3928E-07	7.3912E-07	7.3887E-07	7.3881E-07
Sulfur-36	3.4474E-09	3.4466E-09	3.4465E-09	3.4458E-09	3.4446E-09	3.4443E-09
Chromium-50	1.4357E-03	1.4353E-03	1.4353E-03	1.4350E-03	1.4345E-03	1.4344E-03
Chromium-52	2.7685E-02	2.7679E-02	2.7678E-02	2.7672E-02	2.7663E-02	2.7661E-02
Chromium-53	3.1393E-03	3.1386E-03	3.1385E-03	3.1378E-03	3.1368E-03	3.1365E-03
Chromium-54	7.8143E-04	7.8126E-04	7.8124E-04	7.8107E-04	7.8080E-04	7.8075E-04
Manganese-55	1.2744E-03	1.2741E-03	1.2740E-03	1.2738E-03	1.2733E-03	1.2732E-03
Iron-54	6.8507E-03	6.8492E-03	6.8490E-03	6.8475E-03	6.8452E-03	6.8447E-03
Iron-56	1.0754E-01	1.0752E-01	1.0751E-01	1.0749E-01	1.0745E-01	1.0745E-01
Iron-57	2.4836E-03	2.4831E-03	2.4830E-03	2.4824E-03	2.4816E-03	2.4814E-03
Iron-58	3.3052E-04	3.3045E-04	3.3044E-04	3.3037E-04	3.3025E-04	3.3023E-04
Nickel-58	9.5629E-03	9.5608E-03	9.5605E-03	9.5584E-03	9.5552E-03	9.5545E-03
Nickel-60	3.6836E-03	3.6828E-03	3.6827E-03	3.6819E-03	3.6806E-03	3.6804E-03
Nickel-61	1.6007E-04	1.6004E-04	1.6003E-04	1.6000E-04	1.5994E-04	1.5993E-04

Nickel-62	5.1054E-04	5.1043E-04	5.1042E-04	5.1031E-04	5.1013E-04	5.1009E-04
Nickel-64	1.3002E-04	1.2999E-04	1.2999E-04	1.2996E-04	1.2992E-04	1.2991E-04
Sodium-23	1.0327E-01	1.0336E-01	1.0338E-01	1.0347E-01	1.0362E-01	1.0365E-01

Isotope	400.38	399.58	388.29	358.89	368.44	367.8
Uranium-234	1.1540E-08	1.1540E-08	1.1533E-08	1.1515E-08	1.1521E-08	1.1521E-08
Uranium-235	9.2951E-03	9.2947E-03	9.2893E-03	9.2751E-03	9.2797E-03	9.2794E-03
Uranium-236	1.2706E-06	1.2706E-06	1.2698E-06	1.2679E-06	1.2685E-06	1.2685E-06
Uranium-238	4.5832E-03	4.5830E-03	4.5803E-03	4.5733E-03	4.5756E-03	4.5754E-03
Plutonium-236	4.2341E-16	4.2339E-16	4.2315E-16	4.2250E-16	4.2271E-16	4.2270E-16
Plutonium-238	1.4619E-12	1.4619E-12	1.4610E-12	1.4588E-12	1.4595E-12	1.4595E-12
Plutonium-239	3.5647E-07	3.5645E-07	3.5624E-07	3.5570E-07	3.5588E-07	3.5587E-07
Plutonium-240	1.7051E-11	1.7050E-11	1.7040E-11	1.7014E-11	1.7022E-11	1.7022E-11
Plutonium-241	7.1321E-16	7.1318E-16	7.1276E-16	7.1168E-16	7.1203E-16	7.1200E-16
Plutonium-242	2.0243E-20	2.0242E-20	2.0230E-20	2.0200E-20	2.0210E-20	2.0209E-20
Carbon-12	5.3632E-04	5.3630E-04	5.3598E-04	5.3517E-04	5.3543E-04	5.3541E-04
Silicon-28	1.5110E-03	1.5109E-03	1.5100E-03	1.5077E-03	1.5085E-03	1.5084E-03
Silicon-29	7.6723E-05	7.6720E-05	7.6675E-05	7.6558E-05	7.6596E-05	7.6593E-05
Silicon-30	5.0577E-05	5.0574E-05	5.0545E-05	5.0468E-05	5.0493E-05	5.0491E-05
Phosphorus-31	3.2681E-05	3.2680E-05	3.2660E-05	3.2611E-05	3.2627E-05	3.2626E-05
Sulfur-32	1.6346E-05	1.6345E-05	1.6335E-05	1.6311E-05	1.6319E-05	1.6318E-05
Sulfur-33	1.3086E-07	1.3086E-07	1.3078E-07	1.3058E-07	1.3064E-07	1.3064E-07
Sulfur-34	7.3868E-07	7.3865E-07	7.3822E-07	7.3709E-07	7.3746E-07	7.3743E-07
Sulfur-36	3.4437E-09	3.4436E-09	3.4416E-09	3.4363E-09	3.4380E-09	3.4379E-09
Chromium-50	1.4341E-03	1.4341E-03	1.4332E-03	1.4311E-03	1.4318E-03	1.4317E-03
Chromium-52	2.7656E-02	2.7655E-02	2.7639E-02	2.7596E-02	2.7610E-02	2.7609E-02
Chromium-53	3.1360E-03	3.1358E-03	3.1340E-03	3.1292E-03	3.1308E-03	3.1307E-03
Chromium-54	7.8061E-04	7.8058E-04	7.8012E-04	7.7893E-04	7.7931E-04	7.7929E-04
Manganese-55	1.2730E-03	1.2730E-03	1.2722E-03	1.2703E-03	1.2709E-03	1.2709E-03
Iron-54	6.8435E-03	6.8432E-03	6.8392E-03	6.8287E-03	6.8321E-03	6.8319E-03
Iron-56	1.0743E-01	1.0742E-01	1.0736E-01	1.0720E-01	1.0725E-01	1.0725E-01
Iron-57	2.4810E-03	2.4809E-03	2.4794E-03	2.4756E-03	2.4769E-03	2.4768E-03
Iron-58	3.3017E-04	3.3016E-04	3.2996E-04	3.2946E-04	3.2962E-04	3.2961E-04
Nickel-58	9.5528E-03	9.5524E-03	9.5468E-03	9.5322E-03	9.5370E-03	9.5366E-03
Nickel-60	3.6797E-03	3.6796E-03	3.6774E-03	3.6718E-03	3.6736E-03	3.6735E-03
Nickel-61	1.5990E-04	1.5989E-04	1.5980E-04	1.5956E-04	1.5964E-04	1.5963E-04
Nickel-62	5.1001E-04	5.0999E-04	5.0969E-04	5.0891E-04	5.0916E-04	5.0914E-04
Nickel-64	1.2988E-04	1.2988E-04	1.2980E-04	1.2960E-04	1.2967E-04	1.2966E-04
Sodium-23	1.0372E-01	1.0374E-01	1.0399E-01	1.0464E-01	1.0443E-01	1.0445E-01

Isotope	367.7	367.06	366.05	365.83	365.32	365.19	363.44
Uranium-234	1.1520E-08	1.1520E-08	1.1519E-08	1.1519E-08	1.1519E-08	1.1519E-08	1.1518E-08
Uranium-235	9.2793E-03	9.2790E-03	9.2785E-03	9.2784E-03	9.2782E-03	9.2781E-03	9.2773E-03
Uranium-236	1.2685E-06	1.2684E-06	1.2683E-06	1.2683E-06	1.2683E-06	1.2683E-06	1.2682E-06
Uranium-238	4.5754E-03	4.5753E-03	4.5750E-03	4.5750E-03	4.5749E-03	4.5748E-03	4.5744E-03
Plutonium-236	4.2269E-16	4.2268E-16	4.2266E-16	4.2265E-16	4.2264E-16	4.2264E-16	4.2260E-16
Plutonium-238	1.4595E-12	1.4594E-12	1.4593E-12	1.4593E-12	1.4593E-12	1.4593E-12	1.4591E-12
Plutonium-239	3.5586E-07	3.5585E-07	3.5583E-07	3.5583E-07	3.5582E-07	3.5582E-07	3.5579E-07
Plutonium-240	1.7022E-11	1.7021E-11	1.7020E-11	1.7020E-11	1.7020E-11	1.7019E-11	1.7018E-11
Plutonium-241	7.1200E-16	7.1198E-16	7.1194E-16	7.1193E-16	7.1191E-16	7.1191E-16	7.1184E-16
Plutonium-242	2.0209E-20	2.0208E-20	2.0207E-20	2.0207E-20	2.0206E-20	2.0206E-20	2.0204E-20
Carbon-12	5.3541E-04	5.3539E-04	5.3536E-04	5.3536E-04	5.3534E-04	5.3534E-04	5.3529E-04
Silicon-28	1.5084E-03	1.5084E-03	1.5083E-03	1.5083E-03	1.5082E-03	1.5082E-03	1.5081E-03
Silicon-29	7.6593E-05	7.6590E-05	7.6586E-05	7.6586E-05	7.6584E-05	7.6583E-05	7.6576E-05
Silicon-30	5.0491E-05	5.0489E-05	5.0486E-05	5.0486E-05	5.0484E-05	5.0484E-05	5.0480E-05
Phosphorus-31	3.2625E-05	3.2624E-05	3.2623E-05	3.2622E-05	3.2621E-05	3.2621E-05	3.2618E-05
Sulfur-32	1.6318E-05	1.6317E-05	1.6317E-05	1.6316E-05	1.6316E-05	1.6316E-05	1.6314E-05
Sulfur-33	1.3064E-07	1.3064E-07	1.3063E-07	1.3063E-07	1.3062E-07	1.3062E-07	1.3061E-07
Sulfur-34	7.3743E-07	7.3740E-07	7.3737E-07	7.3736E-07	7.3734E-07	7.3733E-07	7.3727E-07
Sulfur-36	3.4379E-09	3.4378E-09	3.4376E-09	3.4376E-09	3.4375E-09	3.4374E-09	3.4371E-09
Chromium-50	1.4317E-03	1.4317E-03	1.4316E-03	1.4316E-03	1.4315E-03	1.4315E-03	1.4314E-03
Chromium-52	2.7609E-02	2.7608E-02	2.7607E-02	2.7606E-02	2.7606E-02	2.7605E-02	2.7603E-02
Chromium-53	3.1306E-03	3.1305E-03	3.1304E-03	3.1303E-03	3.1303E-03	3.1302E-03	3.1300E-03
Chromium-54	7.7928E-04	7.7926E-04	7.7922E-04	7.7921E-04	7.7919E-04	7.7918E-04	7.7911E-04
Manganese-55	1.2709E-03	1.2708E-03	1.2708E-03	1.2707E-03	1.2707E-03	1.2707E-03	1.2706E-03
Iron-54	6.8319E-03	6.8316E-03	6.8313E-03	6.8312E-03	6.8310E-03	6.8310E-03	6.8303E-03
Iron-56	1.0725E-01	1.0724E-01	1.0724E-01	1.0724E-01	1.0723E-01	1.0723E-01	1.0722E-01
Iron-57	2.4768E-03	2.4767E-03	2.4766E-03	2.4765E-03	2.4765E-03	2.4764E-03	2.4762E-03
Iron-58	3.2961E-04	3.2960E-04	3.2958E-04	3.2958E-04	3.2957E-04	3.2957E-04	3.2954E-04
Nickel-58	9.5366E-03	9.5363E-03	9.5358E-03	9.5357E-03	9.5354E-03	9.5353E-03	9.5345E-03
Nickel-60	3.6735E-03	3.6734E-03	3.6732E-03	3.6731E-03	3.6730E-03	3.6730E-03	3.6727E-03
Nickel-61	1.5963E-04	1.5962E-04	1.5962E-04	1.5961E-04	1.5961E-04	1.5961E-04	1.5959E-04
Nickel-62	5.0914E-04	5.0912E-04	5.0910E-04	5.0909E-04	5.0908E-04	5.0907E-04	5.0903E-04
Nickel-64	1.2966E-04	1.2966E-04	1.2965E-04	1.2965E-04	1.2965E-04	1.2965E-04	1.2963E-04
Sodium-23	1.0445E-01	1.0446E-01	1.0449E-01	1.0449E-01	1.0450E-01	1.0450E-01	1.0454E-01

## B. Results of Density and Cross-Sectional Adjustment

Model Results	$k_{\text{eff}}$
Gradient at 368 with NJOY	1.04577 $\pm$ 0.00008
Gradient at 420 with NJOY	1.04517 $\pm$ 0.00009

Calculated Reactivity Change	Model $\Delta k$	Expected $\Delta k$	Percent Difference
Gradient-to-Gradient	-6.0000E-04	-4.4250E-04	36%

## C. MCNP Input File – Gradient at 420°C

EBR-II Sodium Model

c This model includes 5 axial slices along with 3 nested hexagonal prisms

c with Sodium temperatures ranging from 420.56 to 358.84.

c

c Uses SODIUMdir

c

c Cell Cards

1 300 5.5951E-02 -1 imp:n=1 \$Fuel Lower Extension

30 600 2.4674E-05 -30 imp:n=1 \$Fuel Plenum

3 200 5.6734E-02 -3 imp:n=1 \$Fuel Upper Extension

4 400 5.5951E-02 -4 1 imp:n=1 \$SS Lower Extension

5 400 5.5951E-02 -5 2 30 imp:n=1 \$SS Core Region

6 400 5.5951E-02 -6 3 imp:n=1 \$SS Upper Extension

7 300 5.5951E-02 -7 4 imp:n=1 \$Blanket Lower Extension

8 500 2.9290E-02 -8 5 imp:n=1 \$Blanket Core Region

9 300 5.5951E-02 -9 6 imp:n=1 \$Blanket Upper Extension

c

c Fuel Core Hex Prism Descritization

100 107 1.4039E-01 -1000 -100 imp:n=1 \$Center Hex, Bottom Slice

200 102 1.4030E-01 -1000 100 -200 imp:n=1  
 300 101 1.4027E-01 -1000 200 -300 imp:n=1 \$Center Hex, Center Slice  
 400 102 1.4030E-01 -1000 300 -400 imp:n=1  
 500 107 1.4039E-01 -1000 400 imp:n=1 \$Center Hex, Top Slice  
 c  
 600 105 1.4037E-01 -2000 1000 -100 imp:n=1 \$Middle Hex, Bottom Slice  
 700 103 1.4030E-01 -2000 1000 100 -200 imp:n=1  
 800 104 1.4033E-01 -2000 1000 200 -300 imp:n=1 \$Middle Hex, Center Slice  
 900 103 1.4030E-01 -2000 1000 300 -400 imp:n=1  
 1000 105 1.4030E-01 -2000 1000 400 imp:n=1 \$Middle Hex, Top Slice  
 c  
 1100 108 1.4040E-01 -2 2000 -100 imp:n=1 \$Outer Hex, Bottom Slice  
 1200 106 1.4037E-01 -2 2000 100 -200 imp:n=1  
 1300 109 1.4047E-01 -2 2000 200 -300 imp:n=1 \$Outer Hex, Center Slice  
 1400 106 1.4037E-01 -2 2000 300 -400 imp:n=1  
 1500 108 1.4040E-01 -2 2000 400 imp:n=1 \$Outer Hex, Top Slice  
 c  
 10 0 7 8 9 imp:n=0 \$ Kill Void

c Surface Cards

c Fuel Sections

1 RHP 0 0 0 0 0 60.96 0 56.2137 0 \$Fuel Lower Extension  
 2 RHP 0 0 60.960001 0 0 36.65 0 56.2137 0 \$Fuel Core Region  
 30 RHP 0 0 97.610001 0 0 26.85 0 56.2137 0 \$Plenum  
 3 RHP 0 0 124.460001 0 0 38.1 0 56.2137 0 \$Fuel Upper Extension

c

c SS Sections

4 RHP 0 0 0 0 0 60.96 0 91.86 0 \$SS Lower Extension  
 5 RHP 0 0 60.960001 0 0 63.5 0 91.86 0 \$SS Core Region  
 6 RHP 0 0 124.460001 0 0 38.1 0 91.86 0 \$SS Upper Extension

c

c Blanket Sections

7 RHP 0 0 0 0 0 60.96 0 144.584 0 \$Blanket Lower Extension  
 8 RHP 0 0 60.960001 0 0 63.5 0 144.584 0 \$Blanket Core Region  
 9 RHP 0 0 124.460001 0 0 38.1 0 144.584 0 \$Blanket Upper Extension

c

c Additional Planes to Seperate Sections

c 6 Sections - 12.7 cm each

100 pz 68.62

200 pz 75.62

300 pz 82.95

400 pz 90.28

c

c Additional Inner Hex Prisms to Discretize Core Region

1000 RHP 0 0 60.960001 0 0 36.65 0 23.8155

2000 RHP 0 0 60.960001 0 0 36.65 0 47.6309

c Fuel Core Region

m101 92234.10c 4.5814E-08

92235.10c 3.6901E-02

92236.10c 5.0443E-06

92238.10c 1.8195E-02

94236.10c 1.6809E-15

94238.10c 5.8039E-12

94239.10c 1.4152E-06

94240.10c 6.7690E-11

94241.10c 2.8314E-15

94242.10c 8.0365E-20

6012.50c 4.4067E-04

14028.10c 1.2415E-03

14029.10c 6.3039E-05

14030.10c 4.1556E-05

15031.10c 2.6852E-05

16032.10c 1.3430E-05

16033.10c 1.0752E-07

16034.10c 6.0694E-07

16036.10c 2.8295E-09

24050.10c 1.1784E-03

24052.10c 2.2724E-02

24053.10c 2.5767E-03

24054.10c 6.4139E-04  
25055.10c 1.0460E-03  
26054.10c 5.6229E-03  
26056.10c 8.8268E-02  
26057.10c 2.0385E-03  
26058.10c 2.7129E-04  
28058.10c 7.8490E-03  
28060.10c 3.0234E-03  
28061.10c 1.3138E-04  
28062.10c 4.1905E-04  
28064.10c 1.0672E-04  
11023.10c 8.4762E-02  
m102 92234.10c 4.5805E-08  
92235.10c 3.6895E-02  
92236.10c 5.0434E-06  
92238.10c 1.8192E-02  
94236.10c 1.6806E-15  
94238.10c 5.8028E-12  
94239.10c 1.4149E-06  
94240.10c 6.7678E-11  
94241.10c 2.8309E-15  
94242.10c 8.0351E-20  
6012.50c 4.4059E-04  
14028.10c 1.2413E-03  
14029.10c 6.3028E-05  
14030.10c 4.1549E-05  
15031.10c 2.6847E-05  
16032.10c 1.3428E-05  
16033.10c 1.0750E-07  
16034.10c 6.0683E-07  
16036.10c 2.8290E-09  
24050.10c 1.1782E-03  
24052.10c 2.2719E-02  
24053.10c 2.5762E-03  
24054.10c 6.4127E-04

25055.10c 1.0458E-03  
26054.10c 5.6219E-03  
26056.10c 8.8252E-02  
26057.10c 2.0381E-03  
26058.10c 2.7124E-04  
28058.10c 7.8476E-03  
28060.10c 3.0229E-03  
28061.10c 1.3136E-04  
28062.10c 4.1897E-04  
28064.10c 1.0670E-04  
11023.10c 8.4841E-02  
m103 92234.10c 4.5804E-08  
92235.10c 3.6894E-02  
92236.10c 5.0432E-06  
92238.10c 1.8191E-02  
94236.10c 1.6806E-15  
94238.10c 5.8027E-12  
94239.10c 1.4149E-06  
94240.10c 6.7676E-11  
94241.10c 2.8308E-15  
94242.10c 8.0349E-20  
6012.50c 4.4058E-04  
14028.10c 1.2412E-03  
14029.10c 6.3027E-05  
14030.10c 4.1548E-05  
15031.10c 2.6847E-05  
16032.10c 1.3428E-05  
16033.10c 1.0750E-07  
16034.10c 6.0681E-07  
16036.10c 2.8290E-09  
24050.10c 1.1781E-03  
24052.10c 2.2719E-02  
24053.10c 2.5761E-03  
24054.10c 6.4126E-04  
25055.10c 1.0458E-03

26054.10c 5.6218E-03  
26056.10c 8.8250E-02  
26057.10c 2.0381E-03  
26058.10c 2.7123E-04  
28058.10c 7.8474E-03  
28060.10c 3.0228E-03  
28061.10c 1.3136E-04  
28062.10c 4.1896E-04  
28064.10c 1.0670E-04  
11023.10c 8.4853E-02  
m104 92234.10c 4.5796E-08  
92235.10c 3.6887E-02  
92236.10c 5.0424E-06  
92238.10c 1.8188E-02  
94236.10c 1.6803E-15  
94238.10c 5.8017E-12  
94239.10c 1.4146E-06  
94240.10c 6.7664E-11  
94241.10c 2.8303E-15  
94242.10c 8.0334E-20  
6012.50c 4.4050E-04  
14028.10c 1.2410E-03  
14029.10c 6.3015E-05  
14030.10c 4.1540E-05  
15031.10c 2.6842E-05  
16032.10c 1.3425E-05  
16033.10c 1.0748E-07  
16034.10c 6.0670E-07  
16036.10c 2.8285E-09  
24050.10c 1.1779E-03  
24052.10c 2.2715E-02  
24053.10c 2.5757E-03  
24054.10c 6.4114E-04  
25055.10c 1.0456E-03  
26054.10c 5.6208E-03

26056.10c 8.8234E-02  
26057.10c 2.0377E-03  
26058.10c 2.7118E-04  
28058.10c 7.8460E-03  
28060.10c 3.0223E-03  
28061.10c 1.3133E-04  
28062.10c 4.1889E-04  
28064.10c 1.0668E-04  
11023.10c 8.4933E-02  
m105 92234.10c 4.5783E-08  
92235.10c 3.6877E-02  
92236.10c 5.0409E-06  
92238.10c 1.8183E-02  
94236.10c 1.6798E-15  
94238.10c 5.8000E-12  
94239.10c 1.4142E-06  
94240.10c 6.7645E-11  
94241.10c 2.8296E-15  
94242.10c 8.0312E-20  
6012.50c 4.4038E-04  
14028.10c 1.2407E-03  
14029.10c 6.2998E-05  
14030.10c 4.1529E-05  
15031.10c 2.6834E-05  
16032.10c 1.3422E-05  
16033.10c 1.0745E-07  
16034.10c 6.0654E-07  
16036.10c 2.8277E-09  
24050.10c 1.1776E-03  
24052.10c 2.2708E-02  
24053.10c 2.5750E-03  
24054.10c 6.4096E-04  
25055.10c 1.0453E-03  
26054.10c 5.6192E-03  
26056.10c 8.8209E-02

26057.10c 2.0371E-03  
26058.10c 2.7111E-04  
28058.10c 7.8438E-03  
28060.10c 3.0214E-03  
28061.10c 1.3130E-04  
28062.10c 4.1877E-04  
28064.10c 1.0665E-04  
11023.10c 8.5058E-02  
m106 92234.10c 4.5781E-08  
92235.10c 3.6875E-02  
92236.10c 5.0406E-06  
92238.10c 1.8182E-02  
94236.10c 1.6797E-15  
94238.10c 5.7997E-12  
94239.10c 1.4141E-06  
94240.10c 6.7641E-11  
94241.10c 2.8294E-15  
94242.10c 8.0307E-20  
6012.50c 4.4035E-04  
14028.10c 1.2406E-03  
14029.10c 6.2994E-05  
14030.10c 4.1526E-05  
15031.10c 2.6833E-05  
16032.10c 1.3421E-05  
16033.10c 1.0744E-07  
16034.10c 6.0650E-07  
16036.10c 2.8275E-09  
24050.10c 1.1775E-03  
24052.10c 2.2707E-02  
24053.10c 2.5748E-03  
24054.10c 6.4092E-04  
25055.10c 1.0452E-03  
26054.10c 5.6189E-03  
26056.10c 8.8204E-02  
26057.10c 2.0370E-03

26058.10c 2.7109E-04  
28058.10c 7.8434E-03  
28060.10c 3.0212E-03  
28061.10c 1.3129E-04  
28062.10c 4.1874E-04  
28064.10c 1.0664E-04  
11023.10c 8.5085E-02  
m107 92234.10c 4.5774E-08  
92235.10c 3.6869E-02  
92236.10c 5.0399E-06  
92238.10c 1.8179E-02  
94236.10c 1.6795E-15  
94238.10c 5.7989E-12  
94239.10c 1.4139E-06  
94240.10c 6.7632E-11  
94241.10c 2.8290E-15  
94242.10c 8.0295E-20  
6012.50c 4.4029E-04  
14028.10c 1.2404E-03  
14029.10c 6.2985E-05  
14030.10c 4.1520E-05  
15031.10c 2.6829E-05  
16032.10c 1.3419E-05  
16033.10c 1.0743E-07  
16034.10c 6.0641E-07  
16036.10c 2.8271E-09  
24050.10c 1.1773E-03  
24052.10c 2.2704E-02  
24053.10c 2.5744E-03  
24054.10c 6.4083E-04  
25055.10c 1.0451E-03  
26054.10c 5.6181E-03  
26056.10c 8.8192E-02  
26057.10c 2.0367E-03  
26058.10c 2.7105E-04

28058.10c 7.8422E-03  
28060.10c 3.0208E-03  
28061.10c 1.3127E-04  
28062.10c 4.1868E-04  
28064.10c 1.0663E-04  
11023.10c 8.5149E-02  
m108 92234.10c 4.5772E-08  
92235.10c 3.6868E-02  
92236.10c 5.0397E-06  
92238.10c 1.8179E-02  
94236.10c 1.6794E-15  
94238.10c 5.7987E-12  
94239.10c 1.4139E-06  
94240.10c 6.7629E-11  
94241.10c 2.8289E-15  
94242.10c 8.0293E-20  
6012.50c 4.4027E-04  
14028.10c 1.2404E-03  
14029.10c 6.2983E-05  
14030.10c 4.1519E-05  
15031.10c 2.6828E-05  
16032.10c 1.3418E-05  
16033.10c 1.0743E-07  
16034.10c 6.0639E-07  
16036.10c 2.8270E-09  
24050.10c 1.1773E-03  
24052.10c 2.2703E-02  
24053.10c 2.5743E-03  
24054.10c 6.4081E-04  
25055.10c 1.0450E-03  
26054.10c 5.6179E-03  
26056.10c 8.8188E-02  
26057.10c 2.0367E-03  
26058.10c 2.7104E-04  
28058.10c 7.8420E-03

28060.10c 3.0207E-03  
28061.10c 1.3126E-04  
28062.10c 4.1867E-04  
28064.10c 1.0662E-04  
11023.10c 8.5164E-02  
m109 92234.10c 4.5750E-08  
92235.10c 3.6850E-02  
92236.10c 5.0373E-06  
92238.10c 1.8170E-02  
94236.10c 1.6786E-15  
94238.10c 5.7959E-12  
94239.10c 1.4132E-06  
94240.10c 6.7597E-11  
94241.10c 2.8275E-15  
94242.10c 8.0254E-20  
6012.50c 4.4006E-04  
14028.10c 1.2398E-03  
14029.10c 6.2952E-05  
14030.10c 4.1499E-05  
15031.10c 2.6815E-05  
16032.10c 1.3412E-05  
16033.10c 1.0737E-07  
16034.10c 6.0610E-07  
16036.10c 2.8256E-09  
24050.10c 1.1767E-03  
24052.10c 2.2692E-02  
24053.10c 2.5731E-03  
24054.10c 6.4050E-04  
25055.10c 1.0445E-03  
26054.10c 5.6152E-03  
26056.10c 8.8146E-02  
26057.10c 2.0357E-03  
26058.10c 2.7091E-04  
28058.10c 7.8382E-03  
28060.10c 3.0193E-03

28061.10c 1.3120E-04  
28062.10c 4.1847E-04  
28064.10c 1.0657E-04  
11023.10c 8.5380E-02  
c Fuel Upper Extension  
m200 6012.50c 4.8379E-02  
14028.10c 6.1373E-04  
14029.10c 3.1164E-05  
14030.10c 2.0543E-05  
15031.10c 1.3274E-05  
16032.10c 6.6394E-06  
16033.10c 5.3154E-08  
16034.10c 3.0004E-07  
16036.10c 1.3988E-09  
24050.10c 5.8253E-04  
24052.10c 1.1233E-02  
24053.10c 1.2738E-03  
24054.10c 3.1707E-04  
25055.10c 5.1708E-04  
26054.10c 2.7797E-03  
26056.10c 4.3636E-02  
26057.10c 1.0077E-03  
26058.10c 1.3411E-04  
28058.10c 3.8802E-03  
28060.10c 1.4946E-03  
28061.10c 6.4950E-05  
28062.10c 2.0716E-04  
28064.10c 5.2757E-05  
11023.10c 1.6698E-02  
5010.10c 5.7770E-02  
5011.10c 5.2542E-02  
c Upper and Lower Extension  
m300 6012.50c 1.2663E-03  
14028.10c 3.5674E-03  
14029.10c 1.8115E-04

14030.10c 1.1941E-04  
15031.10c 7.7160E-05  
16032.10c 3.8593E-05  
16033.10c 3.0897E-07  
16034.10c 1.7440E-06  
16036.10c 8.1308E-09  
24050.10c 3.3860E-03  
24052.10c 6.5297E-02  
24053.10c 7.4041E-03  
24054.10c 1.8430E-03  
25055.10c 3.0056E-03  
26054.10c 1.6158E-02  
26056.10c 2.5364E-01  
26057.10c 5.8576E-03  
26058.10c 7.7955E-04  
28058.10c 2.2554E-02  
28060.10c 8.6879E-03  
28061.10c 3.7753E-04  
28062.10c 1.2041E-03  
28064.10c 3.0666E-04  
11023.10c 1.0425E-01  
c Stainless Steel Reflector  
m400 6012.50c 2.2793E-03  
14028.10c 6.4214E-03  
14029.10c 3.2606E-04  
14030.10c 2.1494E-04  
15031.10c 1.3889E-04  
16032.10c 6.9467E-05  
16033.10c 5.5614E-07  
16034.10c 3.1393E-06  
16036.10c 1.4635E-08  
24050.10c 6.0949E-03  
24052.10c 1.1753E-01  
24053.10c 1.3327E-02  
24054.10c 3.3175E-03

25055.10c 5.4101E-03  
26054.10c 2.9084E-02  
26056.10c 4.5655E-01  
26057.10c 1.0544E-02  
26058.10c 1.4032E-03  
28058.10c 4.0598E-02  
28060.10c 1.5638E-02  
28061.10c 6.7956E-04  
28062.10c 2.1674E-03  
28064.10c 5.5198E-04  
11023.10c 2.0849E-02  
c Blanket Core Region  
m500 92234.10c 6.7029E-10  
92235.10c 5.6084E-04  
92236.10c 4.4201E-06  
92238.10c 2.7011E-01  
94236.10c 3.0537E-14  
94238.10c 9.7501E-09  
94239.10c 2.0959E-03  
94240.10c 1.5117E-05  
94241.10c 1.4314E-07  
94242.10c 4.0564E-10  
6012.50c 2.4738E-04  
14028.10c 6.9695E-04  
14029.10c 3.5389E-05  
14030.10c 2.3329E-05  
15031.10c 1.5074E-05  
16032.10c 7.5396E-06  
16033.10c 6.0361E-08  
16034.10c 3.4072E-07  
16036.10c 1.5885E-09  
24050.10c 6.6151E-04  
24052.10c 1.2757E-02  
24053.10c 1.4465E-03  
24054.10c 3.6006E-04

25055.10c 5.8719E-04  
26054.10c 3.1566E-03  
26056.10c 4.9552E-02  
26057.10c 1.1444E-03  
26058.10c 1.5230E-04  
28058.10c 4.4063E-03  
28060.10c 1.6973E-03  
28061.10c 7.3756E-05  
28062.10c 2.3525E-04  
28064.10c 5.9910E-05  
11023.10c 2.4511E-02  
c Plenum Gas  
m600 2003.10c 0.000134  
2004.10c 99.999866  
c kCode  
kcode 100000 1.0 200 1000  
ksrc 0 0 78